Best practices in the characterization of bulk catalyst properties

Jesse Q. Bond [a,*], Eric E. Stangland [b,*], Viktor J. Cybulskis [a,*]

[a] Department of Biomedical and Chemical Engineering, Syracuse University, Syracuse, NY 13244, USA
[b] Core Research and Development, Dow, Inc., Midland, MI 48674, USA

* Corresponding author. *E-mail addresses:*
jqbond@syr.edu (Jesse Q. Bond)
eestangland@dow.com (Eric E. Stangland)
vjcybulskis@syr.edu (Viktor J. Cybulskis)

ABSTRACT

Bulk characterization of a solid provides us with a spatially-averaged description of its physical and chemical properties. These properties are not site-specific, but they are critical for categorizing materials and understanding their catalytic performance. Important bulk chemical properties include elemental composition, crystal structure, atomic coordination environment, and the oxidation states of elements comprising the catalyst. Significant physical properties include accessible surface area, pore volume, pore diameter, and particle size distributions that exist at the various length scales of catalysis. Each physicochemical property is sensitive to the conditions employed for catalyst synthesis, storage, pre-treatment, activation, and characterization. Thus, it is imperative that authors fully describe materials and methods in publications as this metadata provides context for observed phenomena and allows others to recreate the exact conditions that are essential for reproducibility. Such protocols are necessary for a meaningful interpretation of differences in catalyst performance observed across laboratories. This perspective article defines bulk characterization, provides guidance on bulk characterization methods, and emphasizes important considerations and best practices. Our aim is to build a more nuanced understanding of catalyst characterization. We hope that awareness and application of the principles outlined herein will improve rigor and reproducibility in catalysis science.

Keywords: Characterization, Heterogeneous Catalysis, Structure, Chemical Properties, Physical Properties, Best Practices, Rigor and Reproducibility

1. Introduction

Heterogeneous catalysts are complex: they are, in fact, ***heterogeneous***. Historically, this label referred to the fact that solid catalysts exist in a separate phase from gas- and liquid-phase reactants and products, but "heterogeneous" is also (usually) an apt description of a catalyst's physicochemical properties. In general, the catalysts that we purchase and/or synthesize are compositionally and structurally diverse. Catalysis occurs on the accessible surfaces of these materials, and the properties of these surfaces are influenced by the aforementioned heterogeneity. For this reason, accessible surface domains within nominally homogeneous materials, such as γ-Al_2O_3, ZSM-5, or Pt/SiO_2, may show a spatial distribution of reactivities [1-

3]. Frequently, only a small fraction of the accessible surface area, comprised of so-called "active sites," is relevant for catalysis. At a fundamental level, catalysis science aims to identify these active sites, characterize their geometric and electronic structures, and quantify their intrinsic reactivities. This level of insight allows one to map structural descriptions of the active site to quantifiable, macroscale phenomena like reaction rate, fractional conversion, and product selectivity. Such a mapping connects structure to function and provides a sound basis for rational design. Building the insights necessary for informed material design requires tightly coupled ***characterization of the catalyst alongside its performance in catalytic reactors*.** The former (ideally) comprises a description of the physicochemical properties of the catalyst in its working state (i.e., under reaction conditions), while the latter comprises determination of turnover frequencies, apparent kinetic phenomena, and product selectivities.

One can divide the suite of catalyst characterization techniques into "site-specific" methods that resolve the properties of an active site, and "bulk methods" that do not. Rather, bulk methods provide an average description of material properties. They are influenced by material heterogeneity, and they are the focus of this perspective article. We refer readers to related publications that address best practices in active site characterization and the measurement of turnover frequencies [4-9]. Because the bulk properties of a material do not describe an active site, we often dismiss them as kinetically irrelevant; however, proper characterization and reporting of bulk properties is essential for benchmarking, understanding material performance, and establishing consistent synthesis and testing protocols. Moreover, certain bulk properties influence interactions between active sites and adsorbates. This makes them kinetically relevant, so understanding them is critical for resolving observed phenomena [10]. Here, we: (*1*) define bulk properties and distinguish them from site-specific properties, (*2*) discuss the most significant bulk properties in catalysis science, (*3*) outline methods for interrogating bulk properties, (*4*) enumerate challenges associated with each method, and (*5*) establish best practices in performing, interpreting, and discussing bulk characterization.

This perspective is not intended to be prescriptive or comprehensive, nor does it provide exhaustive experimental protocols and methodologies for data analysis. Rather, it presents a set of guiding principles, highlights challenges in solid characterization, and encourages researchers—particularly new practitioners—to consider operating principles and limitations inherent in each technique. It further encourages researchers to report characterization data in a comprehensive and standardized fashion. For those seeking more detailed information about a specific characterization method, several textbooks and review articles introduce fundamental principles and basic applications [11-15].

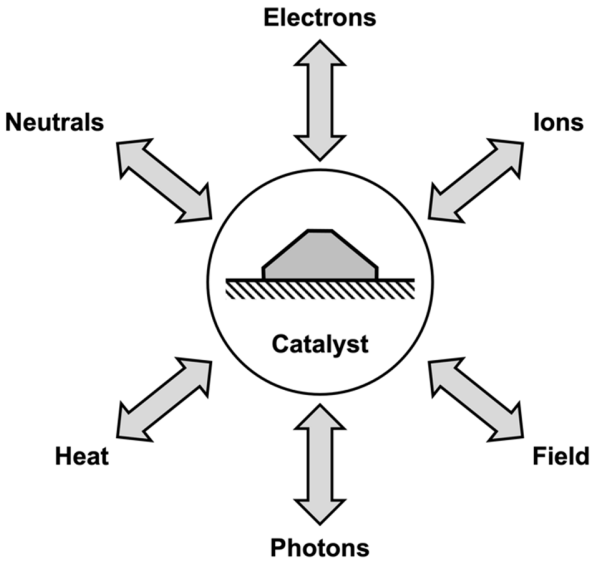

Figure 1. Propst diagram [24] representing various probes used to characterize heterogeneous catalysts. Inward arrows represent excitations and outward arrows represent conveyed information.

Beyond these, experienced practitioners employ in-house protocols that have been refined through years of experimentation and accumulated wisdom [16-18]. Entire volumes have been written about the intricacies of the characterization methods described herein [19-22], and an excellent overview was written by Niemantsverdriet [23]. Readers are encouraged to begin with these resources if they are looking to deepen their understanding of the methods available for characterizing catalytic materials.

1.1 What are bulk properties?

There are numerous techniques for characterizing the physicochemical properties of solids. As illustrated by the Propst diagram [24] in Fig. 1, they can be categorized first by the types of probes that are used to drive excitations (e.g., ions, electrons, photons, heat) and further by the types of information that they provide (e.g., composition, crystal structure, oxidation state, surface area). In a catalysis context, it is useful to further subdivide characterization methods into two categories: (*1*) ***site-specific characterization methods*** that directly interrogate an active/binding site and/or species adsorbed thereupon, and (*2*) ***bulk characterization methods*** that provide composite, averaged information about the material in aggregate. This description is straightforward, but meta-categorization of characterization methods is nuanced. Some nominal "bulk methods" offer site-specific information under carefully controlled conditions; some "bulk properties" are kinetically relevant; and some "site-specific" characterization methods are spatially averaged and influenced by heterogeneity. At the recent NSF and DOE sponsored workshop on *Addressing Rigor and Reproducibility in Heterogeneous, Thermal Catalysis* [4], the authors were struck by the number of discussions that attempted to define bulk properties and bulk characterization methods. We never reached consensus, but the conversations were illuminating. While the central focus of this perspective is best practices in bulk characterization, we first revisit those discussions. They are illustrative, they highlight reasons why reproducibility is elusive, and they underscore complexities and limitations that all of us should consider when characterizing material properties.

A 3-Dimensional Perspective: Active sites on a solid catalyst are confined to its surface. It is thus reasonable to conclude that any characterization method that is not inherently surface sensitive must be a bulk characterization method. Non-surface sensitive techniques *generally* comprise spectroscopies, microscopies, and other characterization methods that leverage probes with substantial penetration depths ($\gtrsim$ 10 nm) and scan large sample areas. As such, these techniques return a volumetric average of material properties in three dimensions, and they are influenced by heterogeneity that exists within the *volume* interrogated. Common examples of volume-averaged techniques include X-ray diffraction (XRD), solid-state magic-angle spinning nuclear magnetic resonance (SS MAS NMR) spectroscopy, routine vibrational spectroscopies (IR, Raman)[1], X-ray absorption spectroscopies (XAS), ultraviolet-visible spectroscopy (UV-Vis), electron microscopy (TEM, SEM), temperature-programmed experiments (TPX), X-Ray

[1]Attenuated total reflectance (ATR) and Diffuse reflectance (DRIFTS) Fourier transform infrared spectroscopies are often described as surface sensitive; however, they have micron-scale penetration depths (~1-10 μm). This means that ATR and DRIFTS are only "surface sensitive" for macroscale domains (e.g., > 1 mm). On the nanometer scales of catalytic surfaces, ATR and DRIFTS are not especially surface sensitive. One can enhance surface sensitivity by using grazing incidence angle IR spectroscopies, but it is unclear if this can rigorously limit penetration depths to below 10 nm.

Fluorescence (XRF), and dissolution-based methods for composition analysis (ICP-OES, ICP-MS, AA).

A 2-Dimensional Perspective: In a catalysis context, the bulk characterization label can (and perhaps should) also apply to many characterization techniques that are historically described as "***surface sensitive***." Classically, this designation stems from the use of probes that have "shallow" penetration depths (e.g., $\lesssim$ 10 nm) [25]. The basic idea is that a shallow penetration depth permits these methods to sample material properties in 2-dimensions without being significantly influenced by underlying bulk structures. Examples of these nominally 2D techniques are low-energy ion scattering (LEIS), low energy electron diffraction (LEED), Auger electron spectroscopy (AES), secondary ion mass spectrometry (SIMS), scanning tunneling microscopy (STM), X-ray photoelectron spectroscopy (XPS), grazing angle spectroscopies (e.g., IR)[1], atomic force microscopy (AFM), scanning tunneling microscopy (STM), and monolayer gas sorption. There are two important caveats. First, the line between "surface sensitive" and "non-surface sensitive" is based on whether a technique has a "shallow" penetration depth. Unfortunately, *"shallow" is an arbitrary and relative quantity*. Its definition changes with: (*1*) the size of the domain interrogated, and (*2*) the material properties of interest. For macroscale samples used in mechanical applications (e.g., $\gtrsim$ 1 mm samples of stainless steel or polyethylene), the outermost 10 nm may well comprise the surface, and probes that penetrate $\lesssim$10 nm can be considered surface sensitive. In contrast, the surface of a solid catalyst is *unambiguously defined as its outermost atomic layer (~ 0.1 nm)*. It is difficult to argue that a characterization method retains surface sensitivity when its penetration ($\lesssim$ 10 nm) depth exceeds this domain size. An example that resonates with most practitioners is the use of XPS for characterizing metal nanoparticles. XPS is widely regarded as surface sensitive since the mean free path of photoelectrons, which is a function of their kinetic energy, is often limited to no more than a few atomic distances through the solid for most metals and metal oxides [23, 26, 27]. However, as one approaches nanoparticle length scales, XPS spectra become increasingly influenced by subsurface atoms. As such, XPS loses its surface sensitivity; it returns a volumetric average of nanoparticle composition and oxidation state; and it effectively becomes a 3D characterization method. A second consideration is that, even if a method provides a true description of 2D surface properties, *surface properties are not the same as site properties*. Outside of single crystals, catalyst surfaces are not uniformly active. Technical catalysts are more often comprised of an expensive active phase (e.g., Pt, Ir, Rh) dispersed on an inexpensive carrier (e.g., SiO_2, Al_2O_3). The metal phase facilitates reactions, but it is undoubtedly a minority component of the surface. This makes certain 2D properties of a material surface-specific but not site-specific; the BET surface area is perhaps the best example of this. BET surface areas are determined by using inert gas physisorption, which occurs on both "active" and "inactive" domains. Because of this, the BET surface area represents a materials *total exposed surface area* as opposed to its *active surface area*; as such, BET surface area is usually a poor approximation for active surface area despite its inherent surface sensitivity. Similar arguments apply for Brønsted acidic bridging hydroxyls in aluminosilicates, coordinatively unsaturated metal cations in Lewis acidic solid oxides, or oxygen vacancies in reducible solid oxides. In such cases, these sites are relatively sparse on an otherwise inert matrix, and BET surface areas will over-estimate the size of the active domain.

A Site-Specific Perspective: Site-specific methods are best viewed as a subset of the more general landscapes described above. One can define site-specific methods as those that are attuned to the active/binding site and are able to resolve its properties and/or its interactions with

adsorbates [9]. Site-specific characterization has two primary goals (though a single method need not address both goals). First, it seeks to *fully describe the geometric and electronic structure of the active site*. Second, it seeks to *quantify the number of accessible active sites in a material*. When paired with rigorous kinetic data, the latter allows one to report turnover frequencies, which are intensive reaction rates that are normalized to a unit active site: they are the gold standard for describing the intrinsic reactivity of a catalyst [5]. With atomic-scale descriptions of structure and reactivity in hand, it is relatively straightforward to correlate structure and function. Thus, site-specific characterization plays a key role in rational design.

The ability to resolve the elements or group of elements that comprise an isolated active site on a solid surface necessitates that site-specific characterization tools are: (*1*) surface sensitive, (*2*) chemically specific, and (*3*) spatially precise at atomic length scales. It is challenging to achieve all three, which means that few characterization methods are rigorously and inherently site-specific. This is especially true in the characterization of technical catalysts that have non-uniform properties. Examples of methods that approach inherent site specificity are STM, which leverages quantum tunneling to provide an atomically resolved map of surface composition and local structure via differences in tunneling current [23, 28], and other high-vacuum techniques that are common in surface science (e.g., LEIS, LEED, HREELS, AES). These methods use ultra-low energy probes that have extremely shallow penetration depths ($\lesssim 1$ nm), which make them especially useful for interrogating surface properties. LEIS is among the most surface sensitive techniques because it uses low energy noble gas ions to drive excitations. This allows it to probe only the outermost atomic layer of a surface to provide information about composition and lattice spacing [29]. Complementary methods, like HREELS and LEED, utilize low energy electrons and probe the first several atomic layers to return electronic spectra and vibrational modes (HREELS) and crystallographic data (LEED) [30]. One drawback of STM and surface science methods is that the dependence on quantum tunneling and/or low energy probes means they can only be performed under challenging experimental conditions (e.g., ultra-high vacuum, cryogenic temperatures). Further, these methods are most meaningful in the analysis of surfaces that are homogeneous and have been rigorously cleaned (oxidation, reduction, sputtering) and annealed so they are devoid of impurities. These methods are therefore best suited to the analysis of pristine single crystals, not powdered catalysts. STM and surface science methods are also expensive, they involve sophisticated equipment and vacuum infrastructure, and they require highly trained operators. For most practitioners, these things mean that the surface science toolkit is available only at additional cost through user facilities, making them inaccessible for routine analysis. As a final note, these methods scan large areas of a sample and are (except for STM) unable to resolve individual surface atoms. This means that they are influenced by compositional and/or structural heterogeneities and therefore return average surface properties akin to other bulk methods.

Site-specific characterization methods are often created by operating less-specialized bulk characterization methods in ways that enhance their surface and chemical specificity. For example, XPS offers innate chemical specificity, but it probes several atomic layers. Routine XPS data are therefore influenced by sub-surface features in, e.g., supported metal catalysts. A potential resolution is to leverage depth profiling to aid in the deconvolution of surface properties from subsurface properties [23, 25, 27]. Alternatively, gas sorption methods can be made site specific by employing titrant molecules that bind selectively at targeted surface atoms. Some common examples include the chemisorption of H_2 or CO on metals to quantify the number of

exposed atoms or the use of hindered pyridines (e.g., 2,6-di-tert-butylpyridine) to selectively titrate Brønsted acid sites on metal oxide surfaces [31-34].

At a minimum, titration methods can be used to determine the quantity of exposed surface atoms or functional groups, but they are versatile and general, and they offer much more than site quantification. When combined with kinetics experiments or other characterization tools, titration methods can also allow one to directly interrogate the role of a specific surface site in the catalytic cycle. Moreover, they can be employed *in situ* to modify and enhance characterization methods in ways that increase site specificity. Even spectroscopies that have large penetration depths, such as X-ray absorption (XAS) and vibrational spectroscopies (IR and Raman), can provide site-specific insights if they are combined with appropriate titrant molecules. Common examples of this include pyridine adsorption coupled with IR spectroscopy to quantify relative populations of Brønsted and Lewis acid sites in metal oxides [35-37], IR spectroscopy of adsorbed CO to probe single atom alloys or to distinguish between different binding sites [38-43], and temperature-programmed desorption (TPD) of alkylamines to quantify Brønsted acid site densities [44-46].

Surface heterogeneity is inevitable in most technical catalysts; this makes it difficult to resolve the structure and function of a single active site (or single type of active site). As an example, metal nanoparticles may have exposed facets (e.g., (100) vs. (111) Miller indices) that exhibit substantially different intrinsic reactivities for a structure-sensitive reaction [47]. The relative populations of these facets can vary with metal particle size [48]. Unfortunately, conventional "site-specific" titration methods, such as static chemisorption of CO or H_2, are unable to resolve edge, corner, step, and terrace sites in the course of site counting. This is because chemisorption methods quantify gas-uptake by tracking barometric changes in the pressure of a gas cell. This offers no information about the solid state, so it is non-trivial to resolve distinct site populations from an adsorption isotherm. The implication is that chemisorption methods *usually* treat geometrically distinct active sites equivalently and return a total site count rather than a site distribution. Similarly, it is common to find Brønsted acid sites confined within the pore structure of zeolites and other microporous materials. These sites may be titrated by small, basic molecules, such as ammonia or ethylamine, and therefore contribute to the "acid site density" measured by ammonia TPD. However, the siting of these acid sites within internal cavities and pores may make them inaccessible to larger substituents, such as highly branched alkenes or bulky aromatics [49-52]. In each above example, naïve interpretation of site titration experiments misrepresents the accessible active surface area, and "turnover frequencies" based thereupon are better viewed as an ensemble-averaged property of all binding sites rather than an intrinsic property of a single active site (i.e., they are essentially a bulk property of the material). In some cases, one can aid the resolution of individual active sites by pairing traditional static chemisorption with an appropriate vibrational spectroscopy. As an example, IR can be used to resolve CO bound on edge, corner, and terrace sites of Pt surfaces.[2]

Is there a clear delineation? It is difficult to articulate a definitive separation between site-specific and bulk 2D or 3D characterization methods. Most attempts to characterize a material result in some degree of spatial averaging and therefore return aggregate properties without resolving compositional and/or structural heterogeneity in active site populations. It is

[2] This is not always feasible with routine spectroscopy. In some cases, such as CO chemisorption on Pt, it is possible to resolve different binding sites using infrared spectroscopy. By contrast, it is difficult to resolve hydrogen adatoms on distinct Pt sites using infrared spectroscopy.

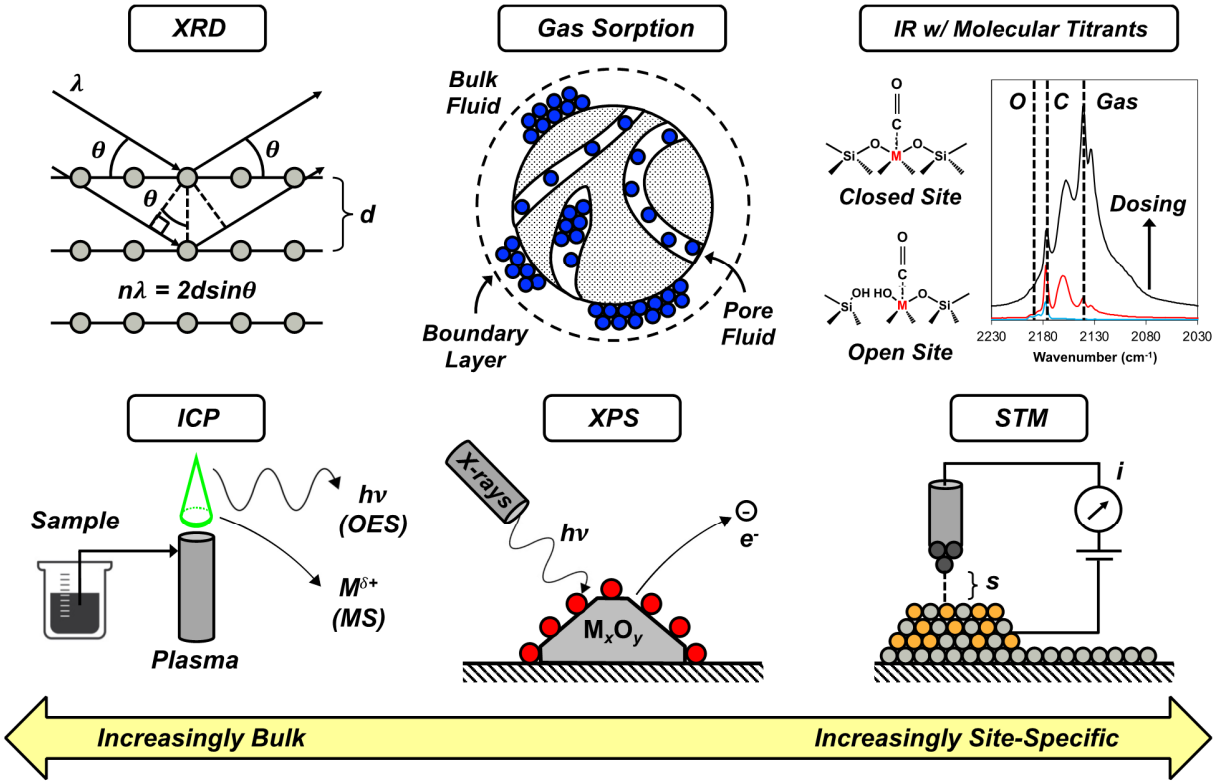

Figure 2. Examples of catalyst characterization methods on continuum ranging from bulk to site-specific.

helpful to view all characterization methods as existing on a continuum wherein one end represents a true bulk 3D property and the other represents a specific property of a single active site (Fig. 2). In some cases, one approaches site-specific insight. An example might include using H_2 chemisorption to quantify the number of active sites on large Pt nanoparticles employed for a structure-insensitive reaction. In this case, turnover frequencies obtained by normalizing reaction rates to hydrogen uptake is a good approximation for the intrinsic activity of a Pt atom. In others, such as using XRD to assess crystallinity and long-range order, one obtains a bulk description of the material in 3D. Often, the information returned lies somewhere between and reflects a convolution of properties. To co-opt a famous euphemism by statistician George E. P. Box "All [descriptions of catalysts and their active sites] are wrong, but some are useful" [53]. We should bear this in mind when performing experiments and interpreting data, especially when we aim to provide an elementary-level description of catalyst performance.

1.2 Why do we care about bulk properties?

A material's bulk properties comprise most of its fingerprint. To a good approximation, the character of solid surfaces and active sites thereupon are determined by atomic composition, bulk crystal structure, and the oxidation state and coordination environment of the elements comprising the material. Bulk properties are therefore important descriptors that help us to categorize materials, understand their behavior, and forecast their performance. As such, accurate and comprehensive reporting of bulk characterization data is critical in identifying the origins of inexplicable or irreproducible behavior observed between laboratories or with changes in synthetic methods. For instance, by identifying TiO_2 samples as anatase, rutile, or mixtures

thereof, one can speak to potential sources of observed variation between nominally identical samples of "titania."

As a straightforward example of bulk property relevance, consider that correct application of methods for dispersing metals and metal oxides onto high surface area carriers, such as incipient wetness impregnation and strong electrostatic adsorption, demand prior insight into bulk properties of the support. These include textural characteristics like specific surface area and pore volume, which influence monolayer loading and the point of incipient wetness [54]. In addition, chemical properties of the support, such as its crystal structure, exposed facets, and/or point of zero charge dictate interactions between metal precursors and the support surface [54, 55]. For these reasons, bulk characterization of a support should always precede attempts to disperse an active phase onto that support.

For a more nuanced example, one might argue that bulk physical properties, such as pore diameter and pore volume, *are* kinetically relevant. In a powdered catalyst, pores and cavities comprise the local environment of the active site, and the effects of confinement and solid solvation become prevalent as cavity dimensions approach molecular length scales [56-61]. These phenomena comprise perturbations to enthalpies, entropies, and free energies that are induced by interactions between reacting species and the pore walls that surround the active site. These interactions can stabilize (or destabilize) transition states and surface intermediates. In doing so, they perturb elementary rate and equilibrium constants and thus overall rates of reaction. Analogously, textural properties can influence selectivity. Micropores span a range of sizes at molecular length scales (0.3-2.0 nm), and it is difficult for large molecules to diffuse through small pores. This makes it possible to restrict the ingress and egress of species based on their kinetic diameter. A classic example is the shape selective production of para-xylene over MFI (~0.6 nm pores) [62, 63] and unidimensional zeolites with 12 member ring pores [64]. Building on this idea, the bulk physical properties of a material control rates of heat, mass, and momentum transfer within a catalyst pellet and throughout a packed bed. Although transport phenomena are not "catalysis" per se, they influence temperature, pressure, and composition in the vicinity of the active site. Thus, understanding transport phenomena allows one to meaningfully interpret observed catalytic activity.

A final point considers the ubiquity and practicality of a characterization method. Bulk characterization methods are often fast, inexpensive, straightforward, and routinely accessible compared to site-specific analogs. It is therefore not surprising that bulk characterization data are among the most reported in the catalysis and materials science literature. The accessibility of bulk characterization methods ensures that this will remain true for the foreseeable future [22, 23]. Although bulk methods will not elucidate isolated active sites, they provide a reliable and holistic description of aggregate material properties. Practitioners should not eschew bulk characterization methods because they are not inherently site-specific; rather, they should understand how to maximally leverage bulk methods and the information that they provide.

2. Discussion

The most significant bulk chemical properties of a material are its elemental composition, its crystal structure(s) or lack thereof, the coordination environment of specific atoms in the material, and the oxidation state(s) of elements comprising the material. We often focus chemical characterization on species intentionally included in the catalyst, but proper characterization also requires that we quantify impurities, which can impact catalyst performance. Important physical

properties include specific surface area and porosity; size distributions for supported metal nanoparticles; grain size distributions for powdered, extruded, or shaped catalysts; bed densities and void volumes; and heat and mass transfer characteristics.

We subsequently divide this article into sections that discuss chemical properties and those that discuss physical properties, and we enumerate relevant characterization methods within each. Throughout, we emphasize an important consideration that applies to all characterization methods and more broadly in catalysis science: *catalyst properties are critically sensitive to the conditions used for its synthesis, storage, pre-treatment, and activation prior to characterization*. Furthermore, its properties are critically sensitive to the conditions employed during characterization. With this in mind, it is easy to see why techniques as ubiquitous as N_2 physisorption to determine BET surface areas can generate tremendous variability in the hands of different practitioners [65]. Because catalyst properties are sensitive to provenance and environment, it is imperative that materials, experimental methods, and procedures for workup and analysis be fully described in publications. In this context, it is worth mentioning that many of the techniques discussed here have already been standardized by the ASTM International Subcommittee D32 under the D32.01 on Physical-Chemical Properties [78]. These standards also outline key metadata that should be included when reporting results obtained using these methods. The community may wish to consider adopting ASTM protocols for characterization and reporting. Where modification is required to fit a specific characterization need, reporting deviations from ASTM protocols and the rationale for said deviations is useful.

2.1.Chemical properties of the catalyst

2.1.1. Elemental composition

Nearly every property of a material stems from its chemical composition, and it is reasonable to expect that two materials with different compositions will perform differently during catalytic testing. The influence of elemental identity and atomic composition is obvious in cases where catalytic function is directly related to a component that is deliberately introduced to the material. For example, consider a hypothetical supported Pt/SiO_2 catalyst wherein Pt is the active phase. Both the atomic percentage and specific properties of Pt are important factors in determining catalyst activity. An increase in Pt loading will usually lead to an increase in Pt surface area, which in turn usually leads to an increase in reaction rate per unit volume of catalyst.[3] To illustrate the significance of elemental identity, one can imagine replacing Pt with an equimolar quantity of Ir. Because Pt and Ir have distinct electronic structures, it is reasonable to expect that this exchange might perturb the reactivity, selectivity, and/or stability of the catalyst [66, 67]. As another example, consider aluminosilicates, which are solid acids comprised of trace, trivalent Al cations incorporated into a SiO_2 matrix. Lattice substitution of Al^{3+} creates Brønsted acidic, bridging surface hydroxyls (Al-OH-Si), and the atomic percentage of Al influences the number of acidic hydroxyls. In general, aluminum-rich materials have more surface acid sites than silicon-rich analogs. Similarly, substituting trivalent B into a SiO_2 matrix creates a borosilicate in which the atomic percentage of B influences the number of acidic

[3] This thought experiment assumes that variations in Pt loading do not impact Pt particle sizes. In reality, increasing Pt loading will lead to some particle growth and loss of metal dispersion. As such, the relationship between specific reaction rate and Pt content is usually less straightforward.

bridging hydroxyls (B-OH-Si). The identity of the trivalent cation is also important because changing the heteroatom substitution from Al^{3+} (aluminosilicate) to B^{3+} (borosilicate) induces a change in electronic structure at the bridging oxygen. The consequence is that Brønsted sites in borosilicates have higher deprotonation energies and are therefore less acidic than analogous sites in aluminosilicates [59, 68]. Finally, combining two or more different metals in an intermetallic or alloy can produce active phases of varying structure and composition that may exhibit substantially different catalytic performance (e.g., Pt vs. Pt_1Zn_1, Pt_1Sn_1 vs. Pt_2Sn_3, Pd vs. PdZn) [69-72]. In all cases, the performance of a material depends both on the identity and the amounts of each "catalytic" element that is intentionally added to the material during synthesis.

Less obvious is the influence of trace elements (impurities) that carry over silently from catalyst synthesis [73]. As a field, our default is usually to ignore impurities—we often do not report purity levels [74], and it is common to see the use of "as received" materials reported in catalysis research. Whether we acknowledge their presence or not, trace impurities impact catalysis by blocking active sites, perturbing electronic structure, and catalyzing unintended reaction pathways. It is therefore reasonable to ask, *"What purity level is adequate to ensure that observed phenomena can be attributed to the intended active phases (e.g., Pt dispersed on SiO_2) rather than to impurities?"* Laboratory grade reagents are frequently purchased at purity levels ranging from 95.0 to > 99.9 wt.% [75, 76]. At the same time, active phases in most catalysts are usually dilute—especially in fundamental, academic research. Supported metals rarely exceed 5 wt.%, and the strong Brønsted acidity of aluminosilicates is predicated upon infrequent substitution of rare Al^{3+} cations into a SiO_2 matrix. For example, some common synthetic zeolites, such as MFI, are categorized as "high silica," meaning that they have Si/Al ratios $\gtrsim 6$ [77-79], where Brønsted acidic hydroxyls comprise less than 5 mol% of the catalyst. This logic extends to base and redox catalysts, where surface active sites—basic O^{2-}, oxygen vacancies, and reducible metal cations—are relatively sparse.

The use of low-grade reagents and lax purification strategies means that residual impurities and contaminants are sometimes present at levels commensurate with the active phase. Without accounting for these species, correct attribution of macroscale observations can be difficult. As an example, Zhu et al. [80, 81] reported that SiO_2 (≥ 99 wt.%) and γ-Al_2O_3 (95-99.997 wt.%) catalyze methanol oxidation and oxidative ketone scission under He. This is observed even though SiO_2 and γ-Al_2O_3 are non-reducible oxides, and it is impossible for them to facilitate oxidative chemistries under He. In this case, the observed activity for both materials must be attributed to reducible oxide impurities (e.g., Fe_2O_3) instead of the nominal solid oxide phase (e.g., SiO_2, γ-Al_2O_3). Another common example is the presence of Fe in aluminosilicates that are prepared using low-purity sources of Si or Al. One concern is that Fe^{3+} is intrinsically Lewis acidic and reducible, which means that Fe_xO_y domains can contribute to observed activity as discussed above [82, 83]. Fe carryover is also important in zeolite synthesis because Fe^{3+} can substitute into an SiO_2 matrix akin to Al^{3+} or B^{3+} [84]. Framework incorporation of Fe^{3+} will create bridging hydroxyls (Fe-OH-Si) with different Brønsted acidity than framework incorporation of Al^{3+} (Al-OH-Si), leading to heterogeneity in the acid site population of the target zeolite [85, 86]. Clearly, "trace impurities" can perturb activity and obscure the intrinsic performance of a material, leading one to report rates or turnover frequencies that are difficult to reproduce. For these reasons, it is important to describe the elemental composition of catalysts in as much detail as possible, noting that it may only take ppm levels of an impurity for it to influence the performance of a catalyst. Some of the most common impurities in metal catalysts and solid oxides are Fe, Si, Al, alkali metals, and halides (or relevant oxides thereof) [87-89]. At

a minimum, practitioners should always screen for these species and disclose their composition in publications.

A major challenge in providing a definitive composition of solids is that there are no reliably quantitative methods for elemental analysis that scan the entire periodic table with uniform precision. Methods that are applicable for lighter metals, such as Li or Na, may not be useful for quantifying rare earth or heavy metals, such as Pb or Bi. Furthermore, one might need entirely different tools to determine carbon content (e.g., CHN analysis, Raman, TPO) as opposed to metal content (e.g., ICP-MS). For these reasons, prior knowledge of the identity and composition of species comprising a solid is essential for selecting appropriate analytical methods, preparing standards, generating calibration curves, and performing quantitative elemental analysis.

There are two useful categories of approaches for determining the elemental composition of solids: X-ray methods and dissolution methods (Table 1). X-ray methods include X-ray fluorescence (XRF) and energy-dispersive X-ray spectroscopy (EDS/EDX/EDAX). These techniques are attractive because they can quickly scan a large composition space to detect the presence of specific elements. X-ray methods can also provide (semi)quantitative information, but this often requires species-specific calibration and detection methods. In general, one should not expect X-Ray methods to simultaneously provide rapid, exploratory analysis and quantitative precision. A more common approach is to first leverage the scanning capabilities of X-ray methods to quickly identify the species present in a sample. Then, more quantitative dissolution-based methods, such as inductively coupled plasma optical emission spectroscopy (ICP-OES), inductively coupled plasma mass spectrometry (ICP-MS), or atomic absorption spectroscopy (AAS) can be used. Dissolution methods are species-specific, and one must approach them with substantial insight into the elements present in the sample and their quantities. These insights are important for two reasons. First, specific elements often require unique strategies for dissolution and stabilization in aqueous media. As an example, one can generally dissolve metal cations at low pH in nitric and/or hydrochloric acid, whereas silicon dissolution requires hydrofluoric acid. Second, detector responses in ICP-OES/MS and AAS vary with the identity of the matrix (i.e., solvent and components therein) and species detected, so unique calibration curves must be prepared for each element of interest in a characteristic matrix.

Table 1
Comparison of common X-ray- and dissolution-based methods for elemental analysis. Adapted from *Characterization of Catalytic Materials* by I.E. Wachs [9].

Criterion	X-ray-based methods		Dissolution-based methods	
	XRF	EDS	ICP-OES	ICP-MS
Elements Detected	B-U	B-U	Li-U (except C, N, O)	Li-U (except C, N, O)
Destructive (Yes/No)	No	No	Yes	Yes
Quantification	Semi-quantitative	Semi-quantitative	Yes, with standards	Yes, with standards
Accuracy	± 1%	± 2%	± 1-10%	± 1-3%
Detection Limits	~1-100 ppm (most elements)	~1,000-10,000 ppm	~ 10 ppb	< 1 ppt
Sample Requirements	Solids, powders, composites (~20-30 mm diameter)	Solids, powders, composites (< 20 mm diameter)	Liquids (2-5 ml), digestible solids (μg-mg of solid)	Solutions, digestible solids, gases, vapors
Main Use	Element identification,	Element identification,	Quantitative composition	Highly sensitive elemental and

	composition, thickness	composition, spatial distribution	measurement over ~5 orders of magnitude	isotopic analysis

2.1.2. Crystal structure

Crystal structure provides a reliable fingerprint for (crystalline) materials. Two materials with identical crystal structures have the same spatial arrangement of atoms and degree of long-range order; therefore, one might reasonably anticipate that these materials will have many similar characteristics. One of the most important aspects of crystallographic analysis is that it can distinguish between crystalline domains present in a sample. This includes differentiating zerovalent metals from their corresponding metal oxides (e.g., Ni vs. NiO); identifying intermetallic compounds (e.g., PtSn vs. Pt_2Sn_3); determining crystalline phases of a single metal (e.g., hcp Pt vs. fcc Pt) or metal oxide (e.g., γ-Al_2O_3 vs. α-Al_2O_3, rutile vs. anatase); distinguishing between different framework geometries of crystalline metal oxides or mixed-metal oxides (e.g., MFI vs. beta zeolites); and uncovering the presence of unintended species in a nominally pure catalyst (e.g., Fe_2O_3 in γ-Al_2O_3). Even if the information is not site-specific, phase identification is useful. For example, one can expect Ni and NiO to perform differently as catalysts because Ni atoms in these two environments have different oxidation states, different lattice spacing, and different electronic structures. Crystallography is especially useful in the preparation of microporous crystalline materials, such as zeolites. In this domain, it is important to understand whether a set of structure-directing agents and synthesis protocols will yield a targeted topology (e.g., MFI, beta, FAU). Significantly, each zeolite framework is characterized by unique pore dimensions, connectivity, and long-range order, each of which is encoded in its crystal structure [90]. For this reason, once the framework topology is identified, one can predict its pore architecture with reasonable certainty [91]. Finally, it is worth noting that even the absence of crystallinity and detection of amorphous regions (when crystallinity is expected) can be helpful in diagnosing the origin of variations in material properties and modifying synthesis parameters [92].

X-ray diffraction (XRD) is the most common method for interrogating a material's crystal structure. Diffraction patterns are produced when X-rays irradiate a crystalline material and subsequently undergo elastic scattering. These patterns are characteristic of a particular material, and they are information rich. First, they permit identification and resolution of a crystal structure. This is accomplished by quantifying diffraction peak locations and their relative intensities, which can be compared with existing databases of reference patterns. Often, materials used in heterogeneous catalysis are comprised of multiple components, each with characteristic crystal structures and diffraction patterns. For example, titanosilicate zeolites, such as Ti-MFI and Ti-beta, contain isolated, tetrahedrally coordinated Ti sites that are isomorphously substituted in framework positions. Framework Ti sites are of interest because they exhibit unique reactivity for various chemistries, such as alkene epoxidation [60, 93-102]. A key synthetic challenge when preparing these materials is avoiding the formation of extra-framework TiO_2 (i.e., anatase, rutile) domains. As shown in Fig. 3, XRD can be used to distinguish between the characteristic MFI and beta frameworks and to identify the presence of bulk TiO_2. Rigorous identification of multiple crystalline domains in complex materials, especially powdered materials, often requires Rietveld refinement, which is a peak fitting method that is commonly applied in the analysis of powder diffraction patterns. Generally, it can be used to deconvolute aggregate XRD patterns into contributions from the individual crystalline domains.

Another consideration is that shifts in XRD peak position relative to established standards are informative as they indicate lattice strain [103, 104]. For this reason, they help one to understand how changes in material composition or synthesis protocol perturb a material's crystal structure. As an example, peak shifts are often observed in XRD patterns upon incorporation of heteroatoms into an otherwise uniform crystalline domain, such as introduction of Al or B into a siliceous zeolite to tune Brønsted acidity. Substitution of the Al or B heteroatom into the framework results in expansion of the zeolite lattice that results in perturbed peak shapes and/or positions relative to the reference pattern for the pure silica material [105]. By characterizing peak shifts induced by these changes, one can assess: (*1*) whether heteroatoms have been incorporated into the framework, (*2*) whether heteroatoms have formed an extra-framework crystalline phase (e.g., γ-Al_2O_3), and (*3*) the degree of lattice expansion or contraction caused by framework incorporation of a heteroatom.

In addition to qualitative information about crystal structure, XRD also provides a quantitative method for assessing the degree of crystallinity in materials that are comprised of crystalline and amorphous domains whose relative populations are determined by the synthesis method. This is accomplished by integrating XRD patterns and normalizing the result to that of a known, crystalline standard. The normalized quantity represents the "degree of crystallinity," which provides a holistic sense of material quality. One useful application of this type of crystallinity analysis is to monitor the extent of demineralization and/or structural collapse that may occur upon exposure of crystalline materials to reaction media [92, 106, 107].

Finally, diffraction patterns can be used to assess the degree of long-range order in a crystalline material and to estimate mean crystallite sizes based on diffraction peak broadening according to the Scherrer equation [108]:

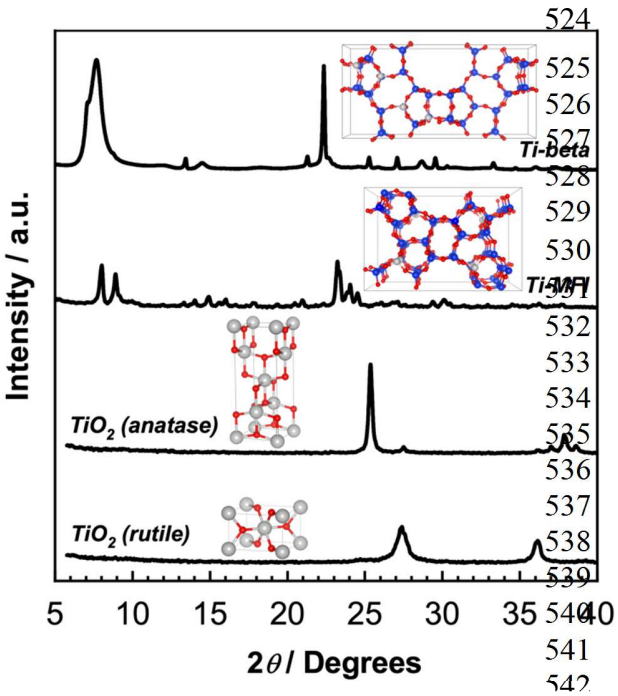

Figure 3. Comparisons of XRD patterns and crystal structures for TiO_2 (rutile), TiO_2 (anatase), Ti-MFI, and Ti-beta. Ti atoms are shown in gray, O atoms in red, and Si atoms in blue.

$$D = \frac{K\lambda}{\beta cos\theta} \quad (1)$$

where D is the mean size of the crystalline domain (nm), K is the dimensionless shape factor (typically 0.9-1), λ is the X-ray wavelength (nm), β is the line broadening at FWHM (radians), and θ is the Bragg angle (radians).

XRD is a robust technique that offers rapid data acquisition. Moreover, it can be used to characterize single crystals, polycrystalline materials, and powdered catalysts with minimal sample preparation. For most cases, one only needs to affix material to a sample holder. X-rays have substantial penetration depth (~10-200 μm) in most materials, with precise values determined by the wavelength of the radiation source, the incident angle, the mass absorption coefficient, and the density and

packing factor for the sample [109, 110]. Importantly, X-ray diffractometers are usually configured to detect scattered hard X-rays (> 5 keV) rather than soft X-rays. Because of this, XRD does not generally require that samples and detectors be placed under high vacuum. As such, there are few restrictions on the use of XRD to probe crystal structures under reaction conditions, such as materials immersed in bulk gas and bulk liquid environments (including water). The latter is especially significant because solid-liquid systems are not generally amenable to *in situ* characterization by using routine IR spectroscopy, electron microscopy, or XPS. Finally, XRD is a relatively inexpensive tool that is easy to use and widely available at universities, national laboratories, and industrial research centers. For this reason, it is one of the primary characterization methods for researchers in the fields of inorganic chemistry, materials science, heterogeneous catalysis, geology, and minerology. Its widespread adoption across numerous fields has supported the development and curation of extensive databases of crystal structures, which are useful in benchmarking and analysis of XRD data. For example, the Inorganic Crystal Structure Database (ISCD) provides a repository of 250k+ structures [111] that can be used along with software tools, such as VESTA [112], to simulate powder XRD patterns and assist in structure assignment. Similarly, the International Zeolite Association's (IZA) Database of Zeolite Structures [90] provides comprehensive structural information on over 250 known zeolite topologies, and it allows users to directly compare experimental powder patterns with calculated and measured XRD patterns for each framework.

A fundamental limitation of XRD is that peak width scales inversely with crystallite size as shown in the Scherrer Equation (Eq. 1). For this reason, it is challenging to use XRD to characterize features at nanometer length scales, which includes the nanoparticles that comprise the active phase in most supported metal catalysts. A common rule of thumb is that lab-based X-ray diffractometers are useful for probing the structure of crystalline domains that are $\gtrsim$ 5-10 nm. Below this point, diffraction peaks become sufficiently broad that they are difficult to resolve with adequate precision. Recent advances in high sensitivity detectors and software tools have made lab-based XRD a viable tool for structural characterization of crystals as small as 1 nm [113, 114]. The caveat in these systems is that metal loadings must be sufficiently high (> 5 wt.%) to generate adequate signal intensity. Another challenge with XRD is that it is not an inherently quantitative method because peak intensity does not scale only with material quantity. Additionally, for nanoscale crystallites in particular, diffuse scattering becomes significant relative to Bragg diffraction and may complicate peak deconvolution [115]. For these reasons, quantitative XRD requires: (*1*) careful instrument calibration to account for intensity drift; (*2*) accurate background subtraction of sample holders, supports, and any non-nanocrystalline material; and (*3*) proper accounting of sample effects, such as absorption, finite thickness, surface roughness, and temperature factors. Finally, it is important to understand that routine crystallography using XRD provides information about 3D crystal structures rather than 2D surface structures, and the two may be substantially different, especially under reaction conditions. This means that crystallography is rarely fully predictive in catalysis. However, surface structure *is* an extension of bulk structure, so it is useful to characterize differences in crystal structure when attempting to explain disparate behaviors observed on different catalyst samples. If surface specific crystallography is of interest, practitioners may wish to consider LEED, which relies on electron diffraction and has a far shallower penetration depth [23].

2.1.3. Oxidation state

The behavior of a catalyst depends on the electronic structure of the elements that comprise it. Characterizing the oxidation state of these elements provides insights about electron density, which is useful in rationalizing data and anticipating performance. Generally, electron density at a surface site determines how strongly species coordinate to that site, the types of elementary steps that occur at that site, and the free energies of activation ($\Delta G^{\ddagger}$) and reaction (ΔG_r°) for these elementary steps. For example, consider the adsorption of ammonia (NH_3) on the surface of a solid oxide, such as γ-Al_2O_3. NH_3 is a basic molecule with a lone pair of electrons on its nitrogen atom that binds strongly at electron deficient sites on the γ-Al_2O_3 surface, namely coordinatively unsaturated Al^{3+} cations [116, 117]. Conversely, NH_3 would bind weakly at basic, electron-rich O^{2-} anions species on γ-Al_2O_3. Insight into species oxidation states also sets expectations for reaction mechanisms and the elementary steps that comprise them. For example, zerovalent transition and platinum group metals (e.g., Ni, Pd, Pt, Ru, Ir) usually facilitate homolytic bond dissociations and single electron processes [118]. In contrast, metal cations in oxide lattices (e.g., Al, Ti, Mo, W, Ce, Sn, V) are Lewis acids that induce heterolytic bond dissociations to generate ionic species, leading to an entirely different cascade of bond scission and bond formation steps than are observed over zerovalent metals [80]. There are two common approaches for assessing oxidation states: X-ray-based methods and temperature-programmed methods. The former directly characterize oxidation states (to a degree), whereas the latter infer oxidation states based on phenomena observed while heating a sample in the presence of a controlled bulk environment.

X-ray Techniques: XRD patterns are characteristic of a material, and one can infer bulk oxidation states from crystallographic data. For example, a phase identified as γ-Al_2O_3 must contain Al^{3+} cations and O^{2-} anions. Analogously, if a diffraction pattern for a Ni/SiO_2 catalyst is dominated by a NiO phase, then one can conclude that Ni is primarily present as Ni^{+2} as opposed to Ni^0. That said, XRD is an indirect way to probe oxidation states, and other X-ray techniques, such as X-ray Absorption Near Edge Spectroscopy (XANES) and XPS, are better attuned to electronic structure and can elucidate variations in electron density that may occur within a given oxidation states. XANES provides bulk-averaged information, whereas XPS, by nature of its limited penetration depth [23, 26, 27] will provide insights about the oxidation states of species within the outermost $\lesssim$ 10 nm of the sample. Comparison of (near) surface oxidation states and bulk oxidation states is useful as the two may vary considerably. This serves as an important reminder that one should not equate bulk structure with surface structure, although it is tempting to do as the former is typically easier to characterize than the latter. Assigning oxidation states in a catalytically relevant surface phase becomes increasingly complex when one considers that oxidation states—especially surface oxidation states—may depend on the environment employed by a specific characterization method. For example, XPS characterization of Pt/SiO_2 might entail collecting spectra associated with Pt 4*f* electrons and Si 2*p* electrons. One would expect that the Pt 4*f* spectra would be sensitive to the environment in the XPS chamber and that those obtained under ultra-high vacuum will differ from those obtained at near ambient pressure under H_2, O_2, or CO. In contrast, Si 2*p* spectra are likely to be similar in each of these environments because Si^{4+} in SiO_2 is unlikely to change oxidation states upon exposure to H_2, CO, or O_2 at conditions that are accessible within an XPS chamber.

Temperature-Programmed Methods: Temperature-programmed experiments (TPX) cannot definitively assign an oxidation state, but they provide useful information regardless. This is especially true when they are combined with X-ray methods or complementary characterization techniques (e.g., thermogravimetric analysis (TGA), vibrational spectroscopy).

The most common TPX methods are temperature-programmed desorption (TPD), temperature-programmed reduction (TPR), and temperature-programmed oxidation (TPO). Each involves heating a catalyst sample under a controlled atmosphere and monitoring the composition of the effluent gas. A TPD experiment comprises the *desorption* of a pre-adsorbed titrant from a catalyst surface while heating the material under an *inert* carrier gas (e.g., N_2, He, Ar) [119, 120]. By contrast, TPO comprises heating a catalyst sample under an *oxidizing* gas blend (e.g., ~1-5% O_2 in N_2, He, or Ar). Finally, TPR involves heating a catalyst sample under a *reducing* gas blend (e.g., ~1-5% H_2 in N_2, He, or Ar) [121]. In TPR and TPO experiments, the use of gas blends is important as they monitor the consumption of H_2 or O_2 based on relative changes in the bulk concentration of H_2 and O_2. These changes are not evident under pure H_2 or O_2 atmospheres; hence, the need for a diluent.

TPD is generally most useful in the context of active site titration, and it does not provide substantial insights into oxidation states or changes in oxidation states. TPR and TPO are better suited to this task as they can provide information about the total number and quantity of reducible elements in a sample. For instance, the reduction of iron oxides could proceed as such:

$$3Fe_2O_3 + H_2 \rightleftharpoons 2Fe_3O_4 + H_2O \quad (2)$$

$$Fe_3O_4 + H_2 \rightleftharpoons 3FeO + H_2O \quad (3)$$

$$FeO + H_2 \rightleftharpoons Fe + H_2O \quad (4)$$

Reduction events and phase changes that occur over the course of a TPR will generally be observed at different temperatures, so careful deconvolution of H_2 consumption profiles *can* provide insight into iron speciation. Moreover, one can quantify the total amount of iron oxide present in a sample from the integrated H_2 consumption over the entire TPR based on the overall stoichiometry:

$$Fe_2O_3 + 3H_2 \rightleftharpoons 2Fe + 3H_2O \quad (5)$$

As in all catalyst characterization, careful sample pre-treatment is crucial for TPX experiments. For high surface area powders especially, it is essential to degas the sample prior to a TPX experiment. This is usually accomplished by heating the catalyst under vacuum or inert gas, which serves to remove H_2O and any other co-adsorbed species. In some cases, it may also be necessary to calcine samples under an oxidizing gas (e.g., air) or to reduce a sample under H_2. Such treatments may be necessary to decompose metal precursors, remove impurities (e.g., carbonaceous deposits, residual Cl), and generate the active phase (e.g., Pt^0, anhydrous V_2O_5). If pre-treatment steps are neglected, H_2O and other contaminants *will* desorb and/or react upon heating and obscure the primary trends of interest, namely reduction or oxidation of the material. As a general rule, the best practice in TPX experiments (as in most characterization experiments) is to employ the same pretreatments used in generating the active phase in catalytic reactors for kinetic analysis.

In theory, any type of flow reactor can be used to perform a TPX experiment (Figure 4): it only needs to be amenable to rapid heating rates (~5-10 K min^{-1}) and permit continuous analysis of the internal or effluent gas composition. That said, it is *best* to operate TPX reactors under conditions where there are no spatial variations in temperature, pressure, or species composition. Examples of gradientless reactors include high vacuum chambers (common in surface science) [122], back-mixed reactors (fluidized beds and spinning basket reactors) [123],

and recycle reactors [124, 125] that are operated at high recycle ratios and low single-pass conversion. The downside of these systems is that each is operationally complex and expensive to fabricate. Because of this, single-pass packed bed reactors are usually employed for TPX experiments. Packed beds are attractive for their cost and simplicity. The tradeoff is that they *always operate under segregated flow without back-mixing*, so they inherently contain axial gradients in composition, temperature, and/or pressure across the reactor. Thus, changes in composition observed across a packed bed reflect a spatial averaging of the effects of composition, temperature, and pressure on reaction kinetics and/or thermodynamics.

As with conventional steady-state kinetic analysis, the best practice for TPX experiments in a packed bed is to operate the system under differential conditions and full kinetic control. Importantly, "differential conditions" are not defined by a threshold value of fractional conversion (e.g., < 10%), which is a common misconception. Differential operation of a packed bed requires that axial gradients in temperature, pressure, and/or composition are sufficiently small that reaction rates can be treated as being spatially invariant. This criterion can be frustratingly difficult to achieve in TPX experiments, where reactor temperatures are ramped over several hundred degrees. This implies that reaction rates will vary by orders-of-magnitude over the course of the experiment, making it very difficult to maintain differential operation and kinetic control throughout. Generally, one must balance catalyst loading, active site density, gas composition, and gas flowrate (i.e., space velocity) to achieve detectable changes in bulk gas composition without inducing transport control or gradients in reaction rate across the catalyst bed. As an example, consider that TPR experiments monitor *changes* in bulk H_2 concentration over the course of a temperature ramp. For this reason, a dilute H_2 stream (1% H_2 in He) is an attractive reducing gas. Because H_2 is present as a minor component, even trace H_2 consumption leads to quantifiable and significant changes in the bulk H_2 mole fraction. A blend of 1% H_2 in He therefore offers good sensitivity in a TPR. However, H_2 consumption is an extensive metric that scales with total H_2 feed rate, mass of catalyst in the packed bed, and density of reducible sites in the catalyst (i.e., μmol g_{cat}^{-1}). If the total H_2 flowrate is low relative to the quantity of reducible metal in the bed, then most or all of the H_2 will be consumed from the gas phase as metal reduction becomes kinetically accessible. This creates a substantial gradient in gas composition across the reactor that: (*1*) violates the differential reactor approximation, (*2*) leads to spatial variation in metal reduction rates, and (*3*) impacts the location and shape of reduction peaks in a TPR. It is also worth considering that it is relatively easy to maintain full kinetic control at low temperatures where reaction rates are low. As temperatures increase, reaction rates will often exceed diffusion rates, shifting the system from kinetic control to transport control. It is important that interpretations of TPX data remain mindful of challenges with maintaining differential operation and kinetic control at elevated temperatures.

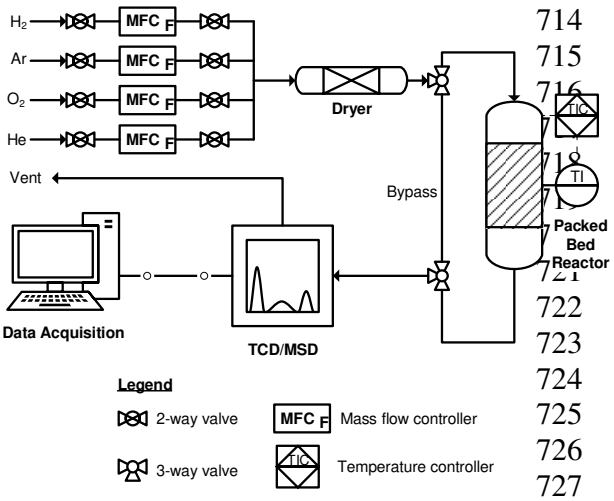

Figure 4. Schematic of an example experimental setup for performing TPX experiments on heterogeneous catalysts.

A major consideration with TPX experiments is the nature of the detector used

to quantify bulk gas compositions. Generally, meaningful data in TPR and TPO experiments is acquired by *continuously* monitoring the reactor effluent gas composition as it evolves on time scales of milliseconds to minutes during the temperature ramp. Thus, routine gas chromatography, which has analysis times $\gtrsim$ 10 minutes, has limited utility in TPX experiments. Instead, one must use analytical techniques that: (*1*) permit identification of individual species in the gas phase, and (*2*) have temporal resolutions of $\lesssim$ 1 second. A common workaround to the chromatography time lag is to equip gas chromatographs with sample trapping loops. This allows one to decouple sampling and analysis time scales; however, these accessories are expensive, and they can be difficult to heat trace, maintain, operate, and calibrate. In theory, spectroscopic methods such as IR, Raman, and UV-vis offer adequate time resolution, but they are often unable to resolve species of interest (i.e., H_2, O_2) with quantitative precision. In practice, the most common approaches for monitoring effluent gas composition on relevant time scales in TPX experiments are mass selective detectors (MSD) and thermal conductivity detectors (TCD).

One advantage of MSDs is that they identify species based on the characteristic mass-to-charge ratios (*m/z*) of molecular fragments produced upon ionization. This feature is especially useful for small molecules, such as H_2 and O_2, which have simple fragmentation patterns. Despite their advantages, MSDs have three notable drawbacks. First, a MSD must operate under vacuum ($\approx 5\text{x}10^{-5}$ mbar), whereas the effluent from a packed bed is typically at or above ambient pressure. Gas monitoring with a MSD is therefore complicated by the need to introduce a high-pressure gas into a vacuum chamber, which requires that one precisely balance gas influx (to the vacuum chamber) with the rate of gas efflux (from the vacuum chamber) to achieve operating pressures of 10^{-4}-10^{-5} mbar. Pressure reduction is usually accomplished with micron-scale capillary tubing or with a leak valve. It is always good practice to heat trace any device used for introducing samples to a vacuum chamber; this is especially true for capillary columns as capillary forces can induce species to condense well below their vapor pressure. At present, turnkey solutions are available for pressure reduction; however, they can be costly (leak valves), cumbersome (capillary tubing), or both. Moreover, the precise balance between gas inflow and outflow will change with the identity of the carrier and the composition of the effluent gas, so it is common to observe variations in the vacuum system pressure with changes in carrier gas over the course of a temperature programmed experiment. Signal from a MSD will scale with the partial pressure of species in the vacuum chamber, so changes in base vacuum pressure give rise to baseline drift over the course of the experiment. A second consideration is that MSDs are subject to imprecisions caused by interferences in fragmentation patterns. For example, H_2O and NH_3 often co-evolve in NH_3 TPD experiments, where the aim is to quantify the NH_3 desorbed. Unfortunately, both NH_3 and H_2O produce fragments at $m/z = 16$ and $m/z = 17$ upon ionization, so neither can be assigned solely to NH_3. In this case, it is important to monitor $m/z = 15$ since it is only produced by the fragmentation of NH_3. Finally, even if one is able to maintain a stable vacuum pressure, MSDs are prone to drift, so, in addition to selecting appropriate *m/z* fragments, extracting quantitative data from a MSD requires frequent calibration and, ideally, an internal standard, such as Ar [75, 80, 81].

TCDs avoid many of the issues that plague MSDs: they operate at ambient pressures, are less susceptible to drift, and are reliably quantitative. The caveat is that a TCD relies on measuring the thermal conductivity of the effluent gas mixture relative to a carrier, which is an average property of the gas mixture that reflects contributions of all species present in the effluent gas as opposed to a single species in the effluent gas. Consequently, TCDs are not species-specific, so they are only useful for binary gas mixtures comprised of an analyte (e.g.,

H_2) in a reference gas (e.g., N_2). For this reason, one must take additional precautions in collecting and interpreting TPX profiles measured with a TCD. To illustrate this point, consider that TPR experiments are commonly used to monitor the reduction of metal oxides based on H_2 consumption, which results in the concomitant generation of H_2O. Unless one takes specific precautions to purify the effluent gas, the signal observed in a TCD detector over the course of a metal oxide TPR is a convolution of H_2 consumption and H_2O generation. A typical remedy is to use a cold trap between the temperature-programmed cell and the TCD detector to condense H_2O and thus quantify only H_2 consumption.

Another important consideration for TPX experiments is that the appropriate choice of carrier gas will change depending on the type of experiment performed and detector used. For example, N_2 is a problematic carrier gas for a MSD that uses electron impact ionization. This type of detector will ionize the N_2 carrier, increasing noise and reducing detector sensitivity. Moreover, N_2 ionization produces fragments at both m/z = 28 and 14. The former is prominent and will interfere with quantitative analysis of molecules such as CO (m/z = 28). In this scenario, He (m/z = 4) is the preferred carrier gas because it does not ionize, which reduces noise and improves sensitivity. It is also easily distinguished from species of interest in TPX experiments. By contrast, He is a poor choice when monitoring H_2 consumption during a TPR experiment with a TCD, which operates by sensing changes in thermal conductivity that occur with changes in gas composition. Thermal conductivities for He (0.15 W m^{-1} K^{-1} at 298K) and H_2 (0.19 W m^{-1} K^{-1} at 298K) are similar, so a TCD has low sensitivity when tracking H_2 consumption from an H_2/He blend. In this scenario, N_2 (0.025 W m^{-1} K^{-1} at 298K) or Ar (0.017 W m^{-1} K^{-1} at 298K) are better choices for the carrier gas. Their thermal conductivities are substantially different from that of H_2, so it is relatively easy to detect even small changes in the bulk H_2 mole fraction and thus quantify H_2 consumption. For a TPO experiment, the converse is true. Because O_2 and N_2 have similar thermal conductivities, it is preferable to employ O_2/He blends when using a TCD to quantify O_2 consumption during a TPO.

An overlooked aspect of temperature-programmed methods is that the catalyst itself undergoes significant chemical changes over the course of the experiment. For example, a TPR reduces the oxidation state of metal cations in a metal oxide by removing oxygen atoms from the lattice and producing water as a product. The implication is that the mass and the crystal structure of the catalyst will both change as the metal oxide is converted into a zerovalent metal. Conversely, a TPO increases the oxidation state of a metal by inserting oxygen atoms into the lattice, which increases the solid mass and shifts the metal crystal structure toward the metal oxide phase. Finally, the nature and existence of surface-bound adsorbates evolves with changes in temperature and gas composition. These changes provide valuable information about the chemical state of the catalyst under specific conditions. Unfortunately, TPX experiments often rely solely on compositional analysis of the effluent gas and are therefore blind to changes in the solid state. Thus, it is useful to couple TPX experiments with complementary methods that can resolve information about the solid catalyst. For example, a TPX experiment can be performed in a TGA unit by monitoring its exhaust composition with a TCD or MSD. The added benefit of the TGA unit is that the sample is held in a quartz crystal microbalance, which permits continuous monitoring of catalyst mass alongside gas composition. This additional information is invaluable in closing mass and element balances, which aids in peak deconvolution to resolve specific oxidation or reduction events. Alternatively, one might perform TPX experiments inside of *in situ* IR, Raman, or XRD cells to probe surface species (IR), metal-oxygen coordination (Raman), or crystal structure (XRD).

Rigorous interpretation of TPX data is challenging. The effluent gas composition profiles observed during a TPX experiment are sensitive to catalyst properties (porosity, metal particle size, active site density, diffusion rates); experimental protocols (ramp rate, space velocity, gas composition); bed properties (void fraction, catalyst mass, bed hydrodynamics, gradients in temperature, pressure, or composition); readsorption of species; and catalyst pretreatment (calcination, reduction, degassing). The practical implication is that specific temperatures where reduction and oxidation events are observed—evidenced by peaks in H_2 or O_2 uptake—can change dramatically with seemingly minor variations in catalyst properties and experimental protocols [126]. Therefore, one must proceed with caution when assigning significance to the location or shape of peaks in H_2 or O_2 consumption observed during TPR and TPO experiments. For example, one might interpret variations in the temperature range of H_2 uptake in a TPR as evidence of differences in reducibility or H_2-spillover. However, such assumptions neglect the influences of many confounding artifacts that can affect rates of H_2 uptake. A more reliable metric is to quantify total H_2 consumption over the course of the TPR by integrating the H_2 uptake curve as a function of time. Total H_2 consumption is not influenced by reduction kinetics, transport phenomena, or hydrodynamics; rather, it is solely a function of the type and quantity of reducible species present in the catalyst bed. These caveats extend to most TPX experiments, urging a cautious interpretation of experimental results by practitioners. For example, desorption peaks observed during NH_3 TPD are routinely assigned to Lewis or Brønsted sites of varying "strength," but this practice is questionable unless it is coupled with spectroscopic analysis. Analogous to TPR and TPO experiments, the most meaningful and reliable metric to report from a TPD experiment is the total quantity of evolved species rather than the temperature associated with a specific desorption event.

2.1.4. Atomic coordination environment

The catalytic nature of an active site is not solely determined by its elemental identity (atomic number) and oxidation state; it is also influenced by the local coordination environment. Specifically, the intrinsic reactivity of an active site is sensitive to the identity of the species that it is bound to. It is also sensitive to the nature of bonds formed with those species. For instance, a Pt atom surrounded by Pt nearest neighbors and next-nearest neighbors can be well-described as having the properties of bulk Pt. In contrast, a Pt atom in a sub-nanometer cluster supported on a metal oxide may have more Pt-O bonds than Pt-Pt bonds, so a Pt atom in this environment is very different from a Pt atom in a single crystal. Alternatively, reducible metal oxides (e.g., oxides of Ce, V, Ti, Mo) are frequently used to facilitate redox chemistries. Often, they are dispersed on high surface area carriers, such as SiO_2 or Al_2O_3, to compensate for the low surface area of the bulk oxide. The mobility of oxygen atoms in the lattice depends on the identity, electronegativity, and reducibility of the species that oxygen atoms are bound to (e.g., V-O-V vs. V-O-Al vs. V-O-Si vs. Ce-O-Si) as well as whether the bonds between the reducible cation and the oxygen are sigma σ(V-O-V) or π(V=O) [127]. Moreover, the reactivities of surface sites on reducible oxides may be sensitive to the extended coordination environment (i.e., the degree of polymerization of the dispersed reducible oxide) [80]. Finally, by probing the coordination environment of catalytic centers, one can identify structural defects, which may play a significant role in the catalytic cycle [128]. Overall, by characterizing coordination environments, we build insights about the physical and chemical structure of the elements comprising a catalyst. In doing so, it is important to recognize that all methods used to interrogate coordination environment are

spatially averaged, and contributions from the surface (where active sites are located) will vary with particle size and loading of the active phase. Unless these tools are combined with appropriate titration methods, they provide a qualitative assessment of the bulk catalyst as opposed to spatially resolved information about an active site.

Numerous tools are available for probing coordination environment. Crystal structures inferred from XRD patterns provide some information about structures adopted by metal cations present in an oxide lattice or metal atoms present in an intermetallic alloy. XAS, specifically extended X-ray absorption fine structure (EXAFS), can also be used to probe the local coordination environment of specific atoms present in the catalyst. One should be aware that EXAFS analysis requires complex deconvolution methods with appropriate references. A detailed discussion of EXAFS is beyond the scope of this overview, and we refer the readers to existing reviews on the topic [23, 129, 130]. SS MAS NMR is frequently used to interrogate the coordination environment of Al and/or Si in aluminosilicates along with framework connectivity and site proximity in zeolites and microporous materials. Thus, it can be useful in assessing material quality and probing for defects in solid oxides containing NMR-active nuclei. Additionally, SS MAS NMR can be used in conjunction with molecular titrants to distinguish and quantify binding sites based on distinct NMR resonances corresponding to unique chemical environments [131, 132]. Vibrational spectroscopies, namely IR and Raman, provide important information as to the bonding environment and chemical structures present in a specific material [37, 39, 133-135]. Where possible, it is advantageous to use IR and Raman in tandem as they are generally suited to probing different bonding environments and so, when coupled, they can provide a more complete picture of the local coordination environment. For example, IR spectroscopy can be used to detect hydroxyl species in bulk oxides, which provides insights into surface acidity and structural defects in silicates and aluminosilicates (e.g., silanol nests). In contrast, Raman is frequently used to detect M-O and M=O bonds in metal oxides, and metal oxide band locations can be used to distinguish between metal cations in different coordination environments [81, 127, 133]. Raman is also particularly useful in characterizing carbons as it can distinguish graphitic and amorphous phases. Finally, DRUV-vis spectroscopy is often used in characterizing the absorption edge energy, or optical band gap, of solid oxides. As shown extensively by Wachs and others [136-140], the edge energy of a solid oxide correlates with its extended coordination environment. Thus, one can employ DRUV-vis to determine the extent of oligomer formation in dispersed solid oxides [80]. DRUV-vis spectroscopy is also frequently employed to distinguish between framework- and non-framework incorporated heteroatoms in crystalline materials (e.g., Ti-MFI, Sn-beta, Ti-beta, Ti-MCM-41) [37, 61, 104, 141, 142], and it can be used to assess the size of metallic domains through changes in resonance with the band gap structure of the nanoparticle.

2.2.Physical properties of the catalyst

2.2.1. Surface area and porosity

Surface area and porosity impact catalysis in many ways ranging from initial synthesis to application in catalytic reactors. Supported catalysts are comprised of an active phase dispersed on high surface area carriers that are, in general, solid materials with extensive macro-, meso-, or microporosity. The surfaces of these pores serve as a support for catalytically active phases, which may include zerovalent metals, metal oxides, organometallics, or even enzymes. Most of these components are introduced to a support using a deposition method such as incipient wetness impregnation, ion exchange, or strong electrostatic adsorption. Assessing surface area and pore volume of the support prior to deposition is necessary to determine, for example, the point of incipient wetness and to forecast the areal density of the active phase in the prepared catalyst. Describing material porosity after synthesis is important because specific surface area and porosity are widely reported for most porous materials; as such, these metrics provide benchmarks that allow one to assess material quality and determine whether a synthesized catalyst is within spec for the intended class of material. As an example, MFI zeolites are expected to have a pore diameter of ~0.6 nm, and siliceous MCM-41 should always have a specific surface area of ~1000 m^2 g^{-1}. Moreover, since pore diameter and tortuosity determine mass transfer characteristics, knowledge of these properties is essential in leveraging established test criteria that permit one to assess the influence of transport phenomena in a catalytic reactor [143]. These include the Weisz-Prater criterion for internal diffusion limitations [144], the effectiveness factor of a catalyst pellet, and Mears' criterion for heat transfer limitations [145]. Each of these correlations invoke numerous physical properties of the catalyst, and they require one to compute a volume-averaged rate of reaction. Accordingly, threshold criteria are heavily dependent on precise determination of catalyst surface area, pore volume, and bulk density. From a reactivity perspective, heterogeneous catalysis is fundamentally a surface phenomenon, so it is always important to quantify the total accessible surface area in catalytic materials as this provides an upper bound on the "active surface area" and thus a lower bound on turnover frequency. Another important consideration is that confinement effects at the nanoscale can fundamentally alter free energies of reaction and activation for elementary steps. These depend critically on cavity dimensions in porous materials, so rigorous quantification of pore volume and pore size distributions is helpful for understanding variations in reactivity observed in samples with similar composition but varying porosity as is often the case with aluminosilicate zeolites.

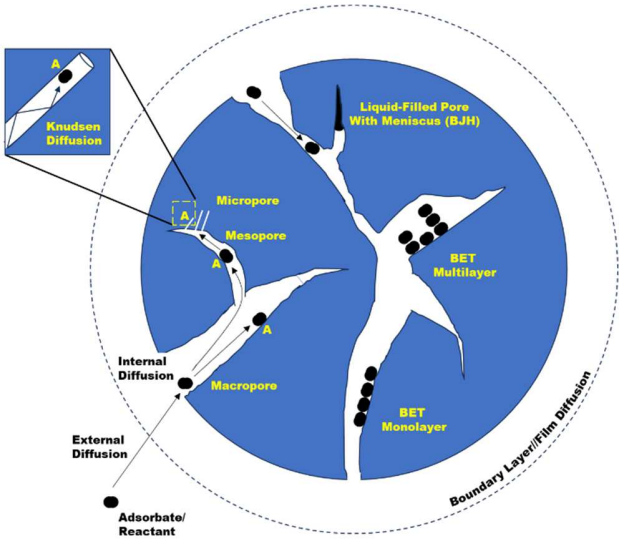

Figure 5. Representation of gas-phase transport and adsorption processes in porous particles of multiple length scales. Physisorption multilayers can occur in larger pores, while site specific (chemi-)sorption can occur on specific sites, represented by A. Liquid-filled pores are possible at critical temperatures and relative pressures.

Fig. 5 schematically describes some simple relationships in the domain for gas-phase molecular transport and adsorption. One can leverage these phenomena in two broad classes of experiments to interrogate porosity: inert gas physisorption and porosimetry. Physisorption is generally useful for characterizing microporosity (~0.3-2.0

nm), mesoporosity (2.0-5.0 nm), and macroporosity up to ~ 50 nm [146], whereas porosimetry is useful for characterizing pore structures ~10 nm-150 μm, which are commonly encountered in pelletized or extruded materials [147].

Gas physisorption: Generally, physisorption experiments involve collecting N_2, Ar, or CO_2 adsorption and desorption isotherms. The choice of adsorbate depends on the material considered and the properties interrogated [148]. More strongly interacting molecules are also suitable for characterization when the situation dictates, though interpretation of the isotherm is generally more nuanced in these cases [149, 150]. N_2 is the most widely used adsorbent, and N_2 physisorption isotherms are usually analyzed in the context of BET and Kelvin pore adsorption theories, which provide a generalized method for characterizing porosity [151, 152]. N_2 physisorption allows a reasonable determination of surface area, total pore volume, average pore diameter, and pore size distributions for most materials; however, its polarizability complicates micropore analysis for materials such as zeolites, carbons, and MOFs [153]. For micropore characterization, Ar and O_2 are preferred adsorbates as they have smaller quadrupole moments than N_2 and so provide a more reliable determination of micropore surface area. Ar and O_2 can otherwise be used to probe the same material properties as N_2 [154]. While it is infrequently used compared to N_2 physisorption, there are few drawbacks to using Ar as an adsorbate. Ar physisorption can be performed at either liquid N_2 (77 K) or liquid Ar (87 K) temperatures, but the use of liquid Ar as a cryostat is preferred as it will give the same pore distribution coverage as the analogous N_2 physisorption experiment. A minor disadvantage is that Ar and liquid Ar are marginally more difficult and expensive to source than N_2 analogs, but the method is usually accessible for most laboratories.

Physisorption experiments rely on barometric data: that is, they record the pressure of a gas phase of known volume that is in equilibrium with a solid sample held at constant temperature. Changes in the gas phase pressure in response to dosing and uptake of an adsorbate are then used to determine the molar quantity of gas adsorbed. This approach is constrained by the capability to resolve changes in pressure that arise from gas adsorption. Total gas uptake scales with surface area, so most instruments require a minimum total solid surface area (~ 5 m^2) to allow for detectable pressure changes and reproducible analysis. Sample cells will generally accommodate maximum solid loadings of ~ 1 g, so it can be challenging to interrogate low surface area materials (i.e., $\lesssim$ 5 m^2 g^{-1}) by conventional physisorption of N_2 or Ar [155]. If sample or system properties prevent one from achieving a total surface area of ~5 m^2, then one should instead consider Kr adsorption at liquid N_2 temperatures for surface area determination [156].

CO_2 is not strictly an inert gas—it has acidic character, and it will bind at basic surface sites like O^{2-} in solid oxides. As such, CO_2 adsorption is less of a general-purpose experiment. That said, CO_2 physisorption at 273 K is a viable alternative for porosity analysis in microporous carbon [157]. For these materials, the kinetics of N_2 and Ar physisorption at cryogenic temperatures are slow, resulting in long equilibration times and protracted physisorption experiments. As isotherms are only reliable if data reflect equilibrium uptake at a given titrant pressure, slow physisorption introduces considerable variability. In these cases, CO_2 physisorption at near-ambient temperature provides a reliable method for interrogating micropore structures. With proper experimental protocols, any of these three adsorbate molecules (N_2, Ar, or CO_2) can be used to build a comprehensive understanding of a material's pore structure [158].

Physisorption isotherms are most informative when they include uptake data from very low relative pressure—$P/P_0 \sim 10^{-6}$ for microporous materials or $P/P_0 \sim 10^{-3}$ for meso- or non-porous samples—up to the saturation pressure of the adsorbate at the temperature where the isotherm is collected, $P/P_0 \sim 1$. Accurate measurement of data at these low-pressure ranges requires proper degassing of the samples, which generally entails heating under vacuum, and may require surprisingly long degas times for samples with extensive microporosity [159]. Furthermore, one can obtain a more complete description of material properties by collecting both adsorption and desorption branches of the isotherm. Specifically, inert gas adsorption and desorption isotherms often show hysteresis. That is to say, the adsorption and desorption processes follow different paths on a graph of gas uptake against relative pressure. Evaluation of hysteresis and other differences in adsorption and desorption branches can reveal important details about the pore structure of a material [160].

The BET method of isotherm analysis has been the gold standard of surface area measurement for nearly 90 years [161]. While the use of BET and other Kelvin equation-derived theories (e.g., Barrett, Joyner, and Halenda (BJH)) is commonplace and built into analysis software for commercial physisorption instruments, significant variation of results from different laboratories is both possible and observed [65]. Users of the BET theory are urged to understand the numerous assumptions that are made [162], to check if the automated fits are appropriate for your data [163], and to use consistency criterion for evaluation of BET-derived parameters [164]. Intuition is also important in model use: when using appropriate models and P/P_0 regions, one should expect to find measured values that align with well-established benchmarks from the literature. For example, HK (Horvath–Kawazoe) analysis of N_2 or Ar adsorption isotherms should return average pore diameters of ~0.6 nm for MFI zeolites. By contrast, BET analysis of N_2 uptake isotherms for hexagonal mesoporous silicas (HMS), such as MCM-41, should return a surface area of ~1000 $m^2\ g^{-1}$ [165]. More modern methods based on nonlocal density functional theory (NLDFT) seek to overcome the limitations of classical theory by using semi-empirical models to determine molecular interaction potentials but they require substantial kernel development [166], although many are available with vendor software [167].

Porosimetry and pyncnometry: Macropore analysis is necessary for a complete description of the porosity and bulk density. This is especially true for pelletized materials that are used in industrial catalysis as they often have pore features on μm-mm length scales. Gas physisorption techniques described in the preceding section are limited to pores smaller than ~50 nm. For macropores larger than 10 nm and up to 150 μm, a complimentary technique – Hg porosimetry – can be used to interrogate the pore structure [147, 151]. Hg porosimetry is an intrusion method governed by the Washburn equation that describes the force required to push a non-wetting fluid into a capillary:

$$D = \frac{-4\gamma \cos\theta}{P} \tag{6}$$

where D is the cylindrical analogue pore diameter, γ is the surface tension, θ is the contact angle, and P is the applied pressure. Through the Washburn equation, the intrusion into a pore of a given size is inversely proportional to the pressure applied. Unlike gas physisorption, which relies on capillary condensation for pore sizing and is therefore limited to micro/mesopore sizes, Hg can directly assess the pore diameter of pores at the meso-macro scale [168, 169]. The toxicity of Hg has made this a technique that is problematic in many laboratories, as spent materials always contain residual Hg in the pores. Reports detail other options and methods

[170], and a standard using H_2O is available [171]. The determination of true skeletal density by He pycnometry [172] or envelope density by powder pycnometry [173] can be used in combination with porosimetry to provide pore volume analysis.

2.2.2. Particle size distributions

Cases of structure sensitivity are well-documented [47], so the size and morphology (e.g., shape) of catalytic domains are important physical properties. It is worth visualizing that the size of the active domain (e.g., a metal nanoparticle) is a different concept from grain size (e.g., a zeolite crystal), which is itself a different concept from the macroscale dimensions of a pelletized material. Each of these domain sizes may influence various aspects of catalyst performance. While variations in the size and shape of metal nanoparticles comprise the classic notion of structure sensitivity, variations in grain sizes or pellet diameters will alter rates of intraparticle and interphase heat and mass transfer. One might also imagine that variations in grain or pellet size may be crucial to achieving workable pressure gradients in large industrial reactors. Ideally, each of these physical dimensions should be characterized and described in publications.

Particle Size Distributions at the Length Scale of the Active Site: Insights from surface science reveal that different metal facets may have different catalytic functions. Often, activity is associated with rare, high-energy corner, edge, or defect sites as opposed to the low index terrace sites that comprise the majority of metal surfaces in large nanoparticles and bulk structures. Conversely, reactivity may be associated with sparse binding sites at metal-support interfaces, as in the case of low-temperature water gas shift [174]. Because interfacial area scales inversely with metal particle size, one might observe that turnover frequencies are influenced by metal dispersion. For these reasons, many reactions should be considered "structure-sensitive" and dependent on both the shape and size of metal particles. It is then important to acknowledge that the shape and size of metal nanoparticles in a typical catalyst is almost certainly non-uniform. In most catalysts, one expects that particle size and structure will vary spatially throughout the catalyst sample. If one accepts that reactions can be size- and structure-sensitive, then one also should expect spatial heterogeneity in reaction rates throughout catalyst pellets. Accordingly, one must not only characterize and report the average size and/or shape of a particle, but also the particle size distribution and heterogeneity in the active phase.

The most common method for obtaining a metal particle size distribution is electron microscopy. For particles at the micron scale, scanning electron microscopy (SEM) and atomic force microscopy (AFM) can be informative. That said, metal catalysis generally occurs on particles between 1-50 nm, which makes scanning and/or transmission electron microscopies (S/TEM) the methods of choice for quantifying the particle size distributions that are most relevant in catalysis. It is worth mentioning that X-ray diffraction, especially with synchrotron-based methods or modern high sensitivity detectors, is now able to detect crystalline domains down to ~1 nm, and peak location/width in diffraction patterns can be used to estimate average metal particle sizes [113, 114]; however, XRD patterns provide no information about particle size distribution and heterogeneity [175-177].

It is challenging to sample a representative set of dispersed metal nanoparticles particles with electron microscopy. As an example, consider a hypothetical catalyst that contains 1 wt.% of hemispherical Pt nanoparticles that have an average diameter of 10 nm and are dispersed onto a high surface area support. The total number of Pt particles found in 1 μg of sample – on the order of one billion – can be estimated from the following equation:

$$N = \frac{12(Wt.\%)\,(m_{cat})}{\pi \rho_{Pt} \langle D_{Pt}^3 \rangle} = \frac{12(1/100)\left(10^{-6}\,g\right)}{\pi\left(21.4\,\frac{g}{cc}\right)(10\,nm)^3} \sim O(10^9) \quad (7)$$

Even with modern automated sampling and counting methods, it is impossible to randomly sample enough particles from this set to obtain a "true" particle size distribution. Moreover, defining a particle size distribution always requires the user to make decisions about how to bin and count particles, which can lead to varied results as multiple users analyze identical micrographs [178]. This uncertainty makes it challenging to, for example, discern mechanisms for sintering that underly catalyst deactivation [179]. Because characterizing a particle size distribution with microscopy is sensitive to specific particles imaged and to choices made by the practitioner, it is important to fully describe the manor and method for obtaining metal particle size distributions.

As a final note, one often considers gas titration of metal surfaces—CO or H_2 chemisorption on Pt for example—to be the gold standard for quantitative determination of exposed metal surface area; however, some metal catalysts are not amenable to straightforward titration methods. In these cases, particle size distributions obtained from microscopy can be used to estimate the accessible metal surface area. This is common practice for gold catalysts and bimetallic alloys, which either lack a reliable chemisorption method or, especially in the case of alloys, may have a poorly defined active site altogether. These surface area calculations are dependent on the determination of a particle size distribution, so they are subject to the same statistical challenges outlined above; as such, reporting recommendations extend to metal surface areas inferred from electron microscopy, and practitioners should report calculations and assumptions used in the generating the particle size distribution and estimating metal surface area from it.

Grain sizes (and distributions) of the bulk catalyst: Beyond the size and distribution of the active phase, the dimensions of the bulk catalyst particle (or pellet) are important to consider as they determine the length scales of diffusion/conduction between the bulk fluid and the active material dispersed throughout the catalyst pellet. In general, larger particles will have larger gradients in temperature and/or species concentration between the center of the pellet and the bulk fluid. In contrast, beds comprised of smaller pellets will have larger pressure gradients. For these reasons, consideration of catalyst macrostructure is critical to reproducibility, especially with engineered materials used in industrial practice. Average grain sizes for powders are relatively easy to determine using sieves [180]. These should generally be reported as part of the catalyst synthesis/testing protocols as they aid in assessing the extent of heat and/or mass transfer limitations. Laser techniques are more sophisticated methods can be utilized to determine particle size distributions at the macroscale (i.e., cm) [181, 182].

3. Perspectives and conclusion

Bulk characterization methods are among the most ubiquitous, practical, and cost-effective techniques available to catalysis practitioners at universities, national laboratories, and industrial research centers. The aggregate property information provided by these methods offers reliable and vital insight into structural and chemical attributes of a catalyst, which are needed to rationalize its kinetic behavior and understand its macroscopic performance. Bulk characterization data are commonly reported in the catalysis literature; unfortunately, catalyst preparation, instrument calibration, control experiments, data analysis, and technique limitations

are not always described in sufficient detail to permit experimental replication and data verification. This oversight makes it challenging to compare results obtained from different laboratories or by using different synthetic protocols, which in turn hinders proper benchmarking of catalyst performance. It is imperative that we, as a community, establish best practices and standards for execution and accurate reporting of bulk characterization data. Doing so will allow us to properly archive knowledge, identify potential origins of inexplicable or irreproducible behavior, and meaningfully interpret differences in catalyst performance.

In this perspective we discuss many useful and widely practiced characterization methods that can be used to assess essential bulk catalyst properties. These methods allow one to interrogate composition, structure, oxidation state, coordination environment, porosity, and particle/grain size distributions. A summary of key takeaways has been condensed into a set of best practices in procedure and reporting (Table 2). We reiterate that this information is not intended to be prescriptive. Our motivation is to encourage catalysis researchers, particularly new entrants in the field, to fully report detailed descriptions of materials and methods along with benchmarking of experimental protocols in their publications to aid in improving rigor and reproducibility in catalysis science.

Table 2
Summary of best practices in procedure and reporting for common characterization methods to assess catalyst bulk properties.

Catalyst property	Common Applications	Concerns or Restrictions	Best Practices and Reporting Recommendations	Useful References
Elemental composition	• Element identification • Composition quantification • Spatial distribution & thickness	• Signal interference by matrix effects • Response overlap for many species • Nonlinear calibration curves • Solubility limits for dissolution methods (acidic vs. alkaline) • HF required for SiO_2 dissolution • XRD and XPS not quantitative	• Calibrate over large range of analyte concentrations • Use internal standards • Include compound of known composition • Match dissolution protocol to target material • List complete reagent specifications (manufacturer, purity, lot number, composition) • Report procedural details to allow replication • Report parameters, settings, procedures used in analysis	[183-187]
Crystal structure	• Assess short- & long-range order • Identify crystal structures & phases • Determine average crystallite sizes • Quantify amounts of each phase present • Detect impurities	• Small (< 5 nm) crystallites difficult to detect • Long-range order does not describe active sites • Careful instrument calibration required for quantification	• Report instrument details (detector type, settings, sample holder & geometry) & calibration procedures • List sample composition, quantity, preparation • Include raw data, peak positions, reference patterns • Prepare figures of sufficient size & resolution to identify impurities	[23, 113, 114]
Oxidation state	• Quantify adsorbed titrants • Assess adsorbate-catalyst interactions • Assess oxidation & reduction susceptibility	• Catalyst age & pre-treatment can introduce large variability in results • Trap H_2O for proper signal integrity • Careful instrument calibration required for quantification • Match gas concentration to sample size • Choose correct detector for experiment • Carrier gas depends on experiment & detector	• Report instrument details (detector type, settings, components) & calibration procedures • List sample composition, quantity, preparation • Report procedural details used in experiment & analysis (ramp rates, hold times) • List complete gas specifications (manufacturer, purity, composition) • Benchmark TPX experiments against standard methods (CaC_2O_4 decomp., CuO reduction)	[23, 126, 188, 189]
Atomic coordination environment	• Characterize M_xO_y networks • Identify bulk coordination environment • Assess oxidation states • Identify atomic species, bonding properties, site	• DRUV-vis spectra of solids often broad and complex • Spectral deconvolution & band assignments are challenging • Band gap assignments require assumptions about transition (spin allowed, spin forbidden, etc.) • Many NMR-active isotopes have low	• Report instrument type, specifications, & settings • Include sample preparation details, age, & pretreatment conditions • Report procedural details used in experiment & analysis (ramp rates, hold times) • Specify how blank/reference spectra acquired	[190, 191]

	proximity	natural abundance • MAS NMR requires special techniques for excitation and registration of signals		
Surface area and porosity	• Determine material surface area, pore size distribution, bulk density, pore volumes • Identify material fractal dimensions	• Results sensitive to pre-treatment conditions • N_2 polarizability complicates micropore analysis • BET and Kelvin theory often misused • Pore size analysis dependent on model • Classical pore size distribution models fail at the capillary limit • Hg is toxic; can alter thin-walled structures (e.g., carbons)	• List sample quantity, form (powder vs. pellet), pre-treatment conditions (pressure, temperature, time) • Report P/P_0 range for isotherm linearization and number of points (single vs. multi-point) • Include thickness model (t-plot, BJH) & corrections to calculations • Report kernel & source for NLDFT analysis • Include full adsorption/desorption isotherms along with the raw data	[18, 151, 163, 169, 171, 192]
Particle and grain size distribution	• Identify catalyst microstructure • Metal cluster size distributions • Element spatial distributions	• Small sample volume relative to bulk • Electron beam-induced particle sintering • Focus on unique rather than ubiquitous features • Metals obscured by support features (e.g., Z-contrast limitations)	• List details of sample preparation and mounting • Include instrument & electron beam characteristics • Report total number of particles analyzed with full distribution curve (not merely averaged statistics)	[11, 176, 177, 180, 182]

1161

Acknowledgements

Funding for the workshop on *Addressing Rigor and Reproducibility in Thermal, Heterogeneous Catalysis* was provided by the National Science Foundation, CBET Division, Catalysis Program under Grant No. 2152559 and the U.S. Department of Energy, Office of Science, Basic Energy Sciences under Award No. DE-SC0022918. The authors thank all workshop participants for sharing the perspectives that have shaped this manuscript. We also thank Neil Schweitzer (Northwestern University) and Robson Schuarca (Amogy) for their helpful feedback on this perspective.

References

[1] A. Bhan, E. Iglesia, A Link between Reactivity and Local Structure in Acid Catalysis on Zeolites, Accounts of Chemical Research, 41 (2008) 559-567.

[2] T. Li, S.-H. Chung, S. Nastase, A. Galilea, Y. Wang, I. Mukhambetov, M. Zaarour, J.C. Navarro de Miguel, J. Cazemier, A. Dokania, L. Panarone, J. Gascon, L. Cavallo, J. Ruiz-Martínez, Influence of active-site proximity in zeolites on Brønsted acid-catalyzed reactions at the microscopic and mesoscopic levels, Chem Catalysis, 3 (2023) 100540.

[3] T.-S. Kim, C.R. O'Connor, C. Reece, Interrogating site dependent kinetics over SiO_2-supported Pt nanoparticles, Nature Communications, 15 (2024) 2074.

[4] N.M. Schweitzer, R. Gounder, R.M. Rioux (Eds.), (2023). Addressing Rigor and Reproducibility in Thermal, Heterogeneous Catalysis (1.00). Zenodo. https://doi.org/10.5281/zenodo.8029159

[5] M. Boudart, Turnover Rates in Heterogeneous Catalysis, Chemical Reviews, 95 (1995) 661-666.

[6] R. Davis, Turnover rates on complex heterogeneous catalysts, AIChE Journal, 64 (2018) 3778-3785.

[7] A. Bhan, W.N. Delgass, Best practices in catalysis: A perspective, Journal of Catalysis, 405 (2022) 419-429.

[8] D.W. Flaherty, A. Bhan, Improving the rigor and reproducibility of catalyst testing and evaluation in the laboratory, Journal of Catalysis, 431 (2024) 115408.

[9] C.J. Wrasman, A.T. Bell, B.D. Chandler, J.W. Harris, S. Kwon, M.R. Ball, S.H. Krishna, S.J. Khatib, P. Bollini, Y. Román-Leshkov, A. "Bean" Getsoian, R.S. Weber, J.A. Lercher, D. Liu, D.E. Resasco, J.S. Bates, J.N. Hall, E.A. Lebrón-Rodríguez, L. Paz Herrera, J.M. Notestein, J.A. Schaidle, Recommendations for improving rigor and reproducibility in site specific characterization, Journal of Catalysis, (2024) 115451.

[10] A. Beck, V. Paunović, J.A. van Bokhoven, Identifying and avoiding dead ends in the characterization of heterogeneous catalysts at the gas–solid interface, Nature Catalysis, 6 (2023) 873-884.

[11] C.N. Satterfield, Heterogeneous Catalysis in Industrial Practice, 2nd ed., Krieger, Malabar, FL, 1996.

[12] C.H. Bartholomew, R.J. Farrauto, Fundamentals of Industrial Catalytic Processes, 2nd ed., John Wiley & Sons, New York, NY, 2011.

[13] M. Boudart, G. Djega-Mariadassou, Kinetics of Heterogeneous Catalytic Reactions, 1st ed., Princeton University Press, Princeton, NJ, 1984.

[14] S. Kelly, W. Sinkler, L. Xu, S. Sanchez, C. Akatay, H. Wang, J.Q. Chen, Advanced characterization for industrial catalysis applications, Chinese Journal of Catalysis, 40 (2019) 1637-1654.
[15] A.C.M. Loy, W.L. Ng, S. Bhattacharya, Advanced characterization techniques for the development of Subatomic scale catalysts: One step closer to industrial scale fabrication, Materials Today Catalysis, 4 (2024) 100033.
[16] Mircromeritics, (2023). Micromeritics Resources Library, https://www.micromeritics.com/resources/library/. Accessed: November 22, 2023.
[17] F.M. Dautzenberg, Ten Guidelines for Catalyst Testing, in: Characterization and Catalyst Development, American Chemical Society, 1989, pp. 99-119.
[18] P.A. Webb, C. Orr, Analytical Methods in Fine Particle Technology, 1st ed., Micromeritics, Norcross, GA, 1997.
[19] J.M. Thomas, R.M. Lambert, Characterization of Catalysts, 1st ed., John Wiley & Sons, Chichester, 1980.
[20] D. Briggs, M.P. Seah, Practical Surface Analysis. Vol. 1, Auger and X-Ray Photoelectron Spectroscopy, 2nd ed., John Wiley & Sons, Chichester, 1990.
[21] W.N. Delgass, G.L. Haller, R. Kellerman, J.H. Lunsford, Spectroscopy in Heterogeneous Catalysis, 1st ed., Academic Press, New York, NY.
[22] I.E. Wachs, Characterization of Catalytic Materials, 1st ed., Butterworth-Heinemann, Stoneham, MA, 1992.
[23] J.W. Niemantsverdriet, Spectroscopy in Catalysis, 3rd ed., Wiley - VCH Verlag GmbH & Co. KGaA, Weinheim, 2007.
[24] R.L. Park, in: R.B. Anderson, P.T. Dawson (Eds.) Experimental Methods in Catalytic Research, Vol. III, Academic Press, New York, NY, pp. 1-36.
[25] F.A. Stevie, C.L. Donley, Introduction to x-ray photoelectron spectroscopy, Journal of Vacuum Science & Technology A, 38 (2020) 1-20.
[26] G.A. Somorjai, Chemistry in Two Dimensions, Surfaces, 1st ed., Cornell University Press, Ithaca, NY, 1981.
[27] D.R. Baer, K. Artyushkova, C. Richard Brundle, J.E. Castle, M.H. Engelhard, K.J. Gaskell, J.T. Grant, R.T. Haasch, M.R. Linford, C.J. Powell, A.G. Shard, P.M.A. Sherwood, V.S. Smentkowski, Practical guides for x-ray photoelectron spectroscopy: First steps in planning, conducting, and reporting XPS measurements, Journal of Vacuum Science & Technology A, 37 (2019).
[28] G. Ertl, Heterogeneous catalysis on atomic scale, Journal of Molecular Catalysis A: Chemical, 182-183 (2002) 5-16.
[29] L.C. Feldman, J.W. Mayer, Fundamentals of Surface and Thin Film Analysis, 1st ed., North-Holland, 1986.
[30] R.F. Egerton, An Introduction to Electron Energy-Loss Spectroscopy, in: R.F. Egerton (Ed.) Electron Energy-Loss Spectroscopy in the Electron Microscope, Springer US, Boston, MA, 1996, pp. 1-29.
[31] P.H. Emmett, S. Brunauer, The use of low temperature van der Waals adsorption isotherms in determining the surface area of iron synthetic ammonia catalysts, Journal of the American Chemical Society, 59 (1937) 1553-1564.
[32] J.H. Sinfelt, D.J.C. Yates, Studies of ethane hydrogenolysis over Group VIII metals: Supported osmium and iron, Journal of Catalysis, 10 (1968) 362-367.

[33] J.J.F. Scholten, A.P. Pijpers, A.M.L. Hustings, Surface Characterization of Supported and Nonsupported Hydrogenation Catalysts, Catalysis Reviews, 27 (1985) 151-206.
[34] J. Macht, C.D. Baertsch, M. May-Lozano, S.L. Soled, Y. Wang, E. Iglesia, Support effects on Bronsted acid site densities and alcohol dehydration turnover rates on tungsten oxide domains, Journal of Catalysis, 227 (2004) 479-491.
[35] A.M. Turek, I.E. Wachs, E. DeCanio, Acidic properties of alumina-supported metal oxide catalysts: an infrared spectroscopy study, Journal of Physical Chemistry, 96 (1992) 5000-5007.
[36] C.A. Emeis, Determination of Integrated Molar Extinction Coefficients for Infrared Absorption Bands of Pyridine Adsorbed on Solid Acid Catalysts, Journal of Catalysis, 141 (1993) 347-354.
[37] J.W. Harris, M.J. Cordon, J.R. Di Iorio, J.C. Vega-Vila, F.H. Ribeiro, R. Gounder, Titration and quantification of open and closed Lewis acid sites in Sn-Beta zeolites that catalyze glucose isomerization, Journal of Catalysis, 335 (2016) 141-154.
[38] K. Ding, A. Gulec, A.M. Johnson, N.M. Schweitzer, G.D. Stucky, L.D. Marks, P.C. Stair, Identification of active sites in CO oxidation and water-gas shift over supported Pt catalysts, Science, 350 (2015) 189-192.
[39] V.J. Cybulskis, J.W. Harris, Y. Zvinevich, F.H. Ribeiro, R. Gounder, A Transmission Infrared Cell Design for Temperature-Controlled Adsorption and Reactivity Studies on Heterogeneous Catalysts, Review of Scientific Instruments, 87 (2016) 103101.
[40] L. DeRita, S. Dai, K. Lopez-Zepeda, N. Pham, G.W. Graham, X.Q. Pan, P. Christopher, Catalyst Architecture for Stable Single Atom Dispersion Enables Site-Specific Spectroscopic and Reactivity Measurements of CO Adsorbed to Pt Atoms, Oxidized Pt Clusters, and Metallic Pt Clusters on TiO_2, Journal of the American Chemical Society, 139 (2017) 14150-14165.
[41] J. Finzel, P. Christopher, Dynamic Pt Coordination in Dilute AgPt Alloy Nanoparticle Catalysts Under Reactive Environments, Topics in Catalysis, 65 (2022) 1587-1603.
[42] V. Giulimondi, S. Mitchell, J. Pérez-Ramírez, Challenges and Opportunities in Engineering the Electronic Structure of Single-Atom Catalysts, ACS Catalysis, 13 (2023) 2981-2997.
[43] R.M. Ferullo, S.A. Fuente, P.G. Belelli, N.J. Castellani, CO interaction with Au atoms adsorbed on terrace, edge and corner sites of the MgO(100) surface. Electronic structure and vibrational analysis from DFT, Surface Science, 603 (2009) 1262-1269.
[44] A.G. Palkhiwala, R.J. Gorte, Characterization of H-FER and H-TON using temperature-programmed desorption of alkylamines, Catalysis Letters, 57 (1999) 19-23.
[45] O.A. Abdelrahman, K.P. Vinter, L. Ren, D. Xu, R.J. Gorte, M. Tsapatsis, P.J. Dauenhauer, Simple quantification of zeolite acid site density by reactive gas chromatography, Catalysis Science & Technology, 7 (2017) 3831-3841.
[46] B.T. Loveless, A. Gyanani, D.S. Muggli, Discrepancy between TPD- and FTIR-based measurements of Brønsted and Lewis acidity for sulfated zirconia, Applied Catalysis B: Environmental, 84 (2008) 591-597.
[47] M. Boudart, G. Djega-Mariadassou, Chapter 5. Structure-Insensitive and Structure-Sensitive Reactions on Metals, in: Kinetics of Heterogeneous Catalytic Reactions, Princeton University Press, Princeton, 1984, pp. 155-193.
[48] R.V. Hardeveld, F. Hartog, The statistics of surface atoms and surface sites on metal crystals, Surface Science, 15 (1969) 189-230.

[49] J.A. Martens, M. Tielen, P.A. Jacobs, J. Weitkamp, Estimation of the void structure and pore dimensions of molecular sieve zeolites using the hydroconversion of n-decane, Zeolites, 4 (1984) 98-107.
[50] J.A. Martens, P.A. Jacobs, The potential and limitations of the n-decane hydroconversion as a test reaction for characterization of the void space of molecular sieve zeolites, Zeolites, 6 (1986) 334-348.
[51] T. Degnan, The implications of the fundamentals of shape selectivity for the development of catalysts for the petroleum and petrochemical industries, Journal of Catalysis, 216 (2003) 32 - 46.
[52] C.Y. Chen, X. Ouyang, S.I. Zones, S.A. Banach, S.A. Elomari, T.M. Davis, A.F. Ojo, Characterization of shape selective properties of zeolites via hydroisomerization of n-hexane, Microporous and Mesoporous Materials, 164 (2012) 71 - 81.
[53] G.E.P. Box, Science and Statistics, Journal of the American Statistical Association, 71 (1976) 791-799.
[54] B.A.T. Mehrabadi, S. Eskandari, U. Khan, R.D. White, J.R. Regalbuto, Chapter One - A Review of Preparation Methods for Supported Metal Catalysts, in: C. Song (Ed.) Advances in Catalysis, Academic Press, 2017, pp. 1-35.
[55] J.W. Geus, Production of Supported Catalysts by Impregnation and (Viscous) Drying, in: Catalyst Preparation, CRC Press, 2006, pp. 341-372.
[56] E.G. Derouane, Molecular Traffic Control and Confinement Catalysis in Molecular Sieves with Differentiated Intersecting Pores, Applied Catalysis A: General, 115 (1994) N2-N3.
[57] E.G. Derouane, J.B. Nagy, C. Fernandez, Z. Gabelica, E. Laurent, P. Maljean, Diffusion of alkanes in molecular sieves evidence for confinement effects, Applied Catalysis, 40 (1988) L1-L10.
[58] D. Fu, Y. Park, M.E. Davis, Confinement effects facilitate low-concentration carbon dioxide capture with zeolites, Proceedings of the National Academy of Sciences, 119 (2022) e2211544119.
[59] A.J. Jones, R.T. Carr, S.I. Zones, E. Iglesia, Acid strength and solvation in catalysis by MFI zeolites and effects of the identity, concentration and location of framework heteroatoms, Journal of Catalysis, 312 (2014) 58-68.
[60] D.T. Bregante, A.M. Johnson, A.Y. Patel, E.Z. Ayla, M.J. Cordon, B.C. Bukowski, J. Greeley, R. Gounder, D.W. Flaherty, Cooperative Effects between Hydrophilic Pores and Solvents: Catalytic Consequences of Hydrogen Bonding on Alkene Epoxidation in Zeolites, Journal of the American Chemical Society, 141 (2019) 7302-7319.
[61] M.J. Cordon, J.W. Harris, J.C. Vega-Vila, J.S. Bates, S. Kaur, M. Gupta, M.E. Witzke, E.C. Wegener, J.T. Miller, D.W. Flaherty, D.D. Hibbitts, R. Gounder, Dominant Role of Entropy in Stabilizing Sugar Isomerization Transition States within Hydrophobic Zeolite Pores, Journal of the American Chemical Society, 140 (2018) 14244-14266.
[62] N.Y. Chen, W.W. Kaeding, F.G. Dwyer, Para-directed aromatic reactions over shape-selective molecular sieve zeolite catalysts, Journal of the American Chemical Society, 101 (1979) 6783-6784.
[63] D. Mitsuyoshi, K. Kuroiwa, Y. Kataoka, T. Nakagawa, M. Kosaka, K. Nakamura, S. Suganuma, Y. Araki, N. Katada, Shape selectivity in toluene disproportionation into para-xylene generated by chemical vapor deposition of tetramethoxysilane on MFI zeolite catalyst, Microporous and Mesoporous Materials, 242 (2017) 118-126.

[64] C.W. Jones, S.I. Zones, M. E. Davis, m-Xylene reactions over zeolites with unidimensional pore systems, Applied Catalysis A: General, 181 (1999) 289-303.
[65] J.W.M. Osterrieth, J. Rampersad, D. Madden, N. Rampal, L. Skoric, B. Connolly, M.D. Allendorf, V. Stavila, J.L. Snider, R. Ameloot, J. Marreiros, C. Ania, D. Azevedo, E. Vilarrasa-Garcia, B.F. Santos, X.-H. Bu, Z. Chang, H. Bunzen, N.R. Champness, S.L. Griffin, B. Chen, R.-B. Lin, B. Coasne, S. Cohen, J.C. Moreton, Y.J. Colón, L. Chen, R. Clowes, F.-X. Coudert, Y. Cui, B. Hou, D.M. D'Alessandro, P.W. Doheny, M. Dincă, C. Sun, C. Doonan, M.T. Huxley, J.D. Evans, P. Falcaro, R. Ricco, O. Farha, K.B. Idrees, T. Islamoglu, P. Feng, H. Yang, R.S. Forgan, D. Bara, S. Furukawa, E. Sanchez, J. Gascon, S. Telalović, S.K. Ghosh, S. Mukherjee, M.R. Hill, M.M. Sadiq, P. Horcajada, P. Salcedo-Abraira, K. Kaneko, R. Kukobat, J. Kenvin, S. Keskin, S. Kitagawa, K.-i. Otake, R.P. Lively, S.J.A. DeWitt, P. Llewellyn, B.V. Lotsch, S.T. Emmerling, A.M. Pütz, C. Martí-Gastaldo, N.M. Padial, J. García-Martínez, N. Linares, D. Maspoch, J.A. Suárez del Pino, P. Moghadam, R. Oktavian, R.E. Morris, P.S. Wheatley, J. Navarro, C. Petit, D. Danaci, M.J. Rosseinsky, A.P. Katsoulidis, M. Schröder, X. Han, S. Yang, C. Serre, G. Mouchaham, D.S. Sholl, R. Thyagarajan, D. Siderius, R.Q. Snurr, R.B. Goncalves, S. Telfer, S.J. Lee, V.P. Ting, J.L. Rowlandson, T. Uemura, T. Iiyuka, M.A. van der Veen, D. Rega, V. Van Speybroeck, S.M.J. Rogge, A. Lamaire, K.S. Walton, L.W. Bingel, S. Wuttke, J. Andreo, O. Yaghi, B. Zhang, C.T. Yavuz, T.S. Nguyen, F. Zamora, C. Montoro, H. Zhou, A. Kirchon, D. Fairen-Jimenez, How Reproducible are Surface Areas Calculated from the BET Equation?, Advanced Materials, 34 (2022) 2201502.
[66] R.R. Davda, J.W. Shabaker, G.W. Huber, R.D. Cortright, J.A. Dumesic, Aqueous-phase reforming of ethylene glycol on silica-supported metal catalysts, Applied Catalysis B: Environmental, 43 (2003) 13-26.
[67] D.W. Flaherty, E. Iglesia, Transition-State Enthalpy and Entropy Effects on Reactivity and Selectivity in Hydrogenolysis of n-Alkanes, Journal of the American Chemical Society, 135 (2013) 18586-18599.
[68] A.N. Petelski, N.M. Peruchena, M.F. Zalazar, Acidity of Isomorphic Substituted Zeolites with B, Al and Ga Revisited, ChemPhysChem, (2024) doi.org/10.1002/cphc.202400080.
[69] C. Ye, M. Peng, Y. Wang, N. Zhang, D. Wang, M. Jiao, J.T. Miller, Surface Hexagonal Pt_1Sn_1 Intermetallic on Pt Nanoparticles for Selective Propane Dehydrogenation, ACS Applied Materials & Interfaces, 12 (2020) 25903-25909.
[70] X. Yang, B.E. Koel, Adsorption and Reaction of Unsaturated Hydrocarbons on Sn/Pt Alloys, in: K. Wandelt (Ed.) Encyclopedia of Interfacial Chemistry, Elsevier, Oxford, 2018, pp. 1-10.
[71] V.J. Cybulskis, B.C. Bukowski, H.-T. Tseng, J.R. Gallagher, Z. Wu, E. Wegener, A.J. Kropf, B. Ravel, F.H. Ribeiro, J. Greeley, J.T. Miller, Zinc Promotion of Platinum for Catalytic Light Alkane Dehydrogenation: Insights into Geometric and Electronic Effects, ACS Catalysis, 7 (2017) 4173-4181.
[72] P. Ticali, S. Morandi, G. Shterk, S. Ould-Chikh, A. Ramirez, J. Gascon, S.-H. Chung, J. Ruiz-Martinez, S. Bordiga, PdZn/ZrO_2+SAPO-34 bifunctional catalyst for CO_2 conversion: Further insights by spectroscopic characterization, Applied Catalysis A: General, 655 (2023) 119100.
[73] L.-C. Wang, M.L. Personick, S. Karakalos, R. Fushimi, C.M. Friend, R.J. Madix, Active sites for methanol partial oxidation on nanoporous gold catalysts, Journal of Catalysis, 344 (2016) 778-783.

[74] O.A. Abdelrahman, H.Y. Luo, A. Heyden, Y. Román-Leshkov, J.Q. Bond, Toward rational design of stable, supported metal catalysts for aqueous-phase processing: Insights from the hydrogenation of levulinic acid, Journal of Catalysis, 329 (2015) 10-21.
[75] J.Q. Bond, C.S. Jungong, A. Chatzidimitriou, Microkinetic analysis of ring opening and decarboxylation of γ-valerolactone over silica alumina, Journal of Catalysis, 344 (2016) 640-656.
[76] X. Gao, A. Heyden, O.A. Abdelrahman, J.Q. Bond, Microkinetic analysis of acetone hydrogenation over Pt/SiO_2, Journal of Catalysis, 374 (2019) 183-198.
[77] A.W. Burton, S.I. Zones, Chapter 5 - Organic Molecules in Zeolite Synthesis: Their Preparation and Structure-Directing Effects, in: J. Čejka, H. van Bekkum, A. Corma, F. Schüth (Eds.) Stud Surf Sci Catal, Elsevier, 2007, pp. 137-179.
[78] W.E. Farneth, R.J. Gorte, Methods for Characterizing Zeolite Acidity, Chemical Reviews, 95 (1995) 615-635.
[79] R.F. Lobo, S.I. Zones, M.E. Davis, Structure-direction in zeolite synthesis, Journal of Inclusion Phenomena and Molecular Recognition in Chemistry, 21 (1995) 47-78.
[80] R. Zhu, B. Liu, S. Wang, X. Huang, R.L. Schuarca, W. He, V.J. Cybulskis, J.Q. Bond, Understanding the mechanism(s) of ketone oxidation on VO_x/γ-Al_2O_3, Journal of Catalysis, 404 (2021) 109-127.
[81] R. Zhu, A. Chatzidimitriou, J.Q. Bond, Influence of vanadate structure and support identity on catalytic activity in the oxidative cleavage of methyl ketones, Journal of Catalysis, 359 (2018) 171-183.
[82] F. Domka, A. Basińska, W. Przystajko, R. Fiedorow, Surface chemistry of Fe_2O_3-Cr_2O_3 and Fe_2O_3 catalysts, Surface Technology, 21 (1984) 101-108.
[83] S. Zhou, B. Shao, W. Jin, X. Li, Y. Ding, B. Wang, Y. Kong, Acid-redox bifunctional Fe/Al-AMS catalyst: Simultaneously oriented introducing Fe2O3 in the channels and Al in the framework of AMS and its enhanced catalytic performance, Applied Catalysis A: General, 575 (2019) 159-169.
[84] J. Zhang, X. Tang, H. Yi, Q. Yu, Y. Zhang, J. Wei, Y. Yuan, Synthesis, characterization and application of Fe-zeolite: A review, Applied Catalysis A: General, 630 (2022) 118467.
[85] Y. Xu, J. Liu, G. Ma, J. Wang, J. Lin, H. Wang, C. Zhang, M. Ding, Effect of iron loading on acidity and performance of Fe/HZSM-5 catalyst for direct synthesis of aromatics from syngas, Fuel, 228 (2018) 1-9.
[86] M. Baranak, B. Gürünlü, A. Sarıoğlan, Ö. Ataç, H. Atakül, Low acidity ZSM-5 supported iron catalysts for Fischer–Tropsch synthesis, Catalysis Today, 207 (2013) 57-64.
[87] A.S. Asundi, A.S. Hoffman, S.S. Nathan, A. Boubnov, S.R. Bare, S.F. Bent, Impurity Control in Catalyst Design: The Role of Sodium in Promoting and Stabilizing Co and Co_2C for Syngas Conversion, ChemCatChem, 13 (2021) 1186-1194.
[88] A. Staerz, H.G. Seo, T. Defferriere, H.L. Tuller, Silica: ubiquitous poison of metal oxide interfaces, Journal of Materials Chemistry A, 10 (2022) 2618-2636.
[89] I. Spanos, J. Masa, A. Zeradjanin, R. Schlögl, The Effect of Iron Impurities on Transition Metal Catalysts for the Oxygen Evolution Reaction in Alkaline Environment: Activity Mediators or Active Sites?, Catalysis Letters, 151 (2021) 1843-1856.
[90] C. Baerlocher, L.B. McCusker, (2023). Database of Zeolite Structures, http://www.iza-structure.org/databases. Accessed: November 22, 2023.

[91] R.E. Morris, P.S. Wheatley, Chapter 11 - Diffraction Techniques Applied to Zeolites, in: J. Čejka, H. van Bekkum, A. Corma, F. Schüth (Eds.) Stud Surf Sci Catal, Elsevier, 2007, pp. 375-IX.
[92] R.M. Ravenelle, F. Schüβler, A. D'Amico, N. Danilina, J.A. van Bokhoven, J.A. Lercher, C.W. Jones, C. Sievers, Stability of Zeolites in Hot Liquid Water, Journal of Physical Chemistry C, 114 (2010) 19582-19595.
[93] J.W. Harris, J. Arvay, G. Mitchell, W.N. Delgass, F.H. Ribeiro, Propylene Oxide Inhibits Propylene Epoxidation over Au/TS-1, Journal of Catalysis, 365 (2018) 105-114.
[94] M. Haruta, B.S. Uphade, S. Tsubota, A. Miyamoto, Selective Oxidation of Propylene over Gold Deposited on Titanium-Based Oxides, Research on Chemical Intermediates, 24 (1998) 329-336.
[95] W.-S. Lee, M. Cem Akatay, E.A. Stach, F.H. Ribeiro, W. Nicholas Delgass, Reproducible Preparation of Au/TS-1 with High Reaction Rate for Gas Phase Epoxidation of Propylene, Journal of Catalysis, 287 (2012) 178-189.
[96] W.-S. Lee, M. Cem Akatay, E.A. Stach, F.H. Ribeiro, W. Nicholas Delgass, Enhanced Reaction Rate for Gas-Phase Epoxidation of Propylene using H2 and O2 by Cs Promotion of Au/TS-1, Journal of Catalysis, 308 (2013) 98-113.
[97] T.A. Nijhuis, B.J. Huizinga, M. Makkee, J.A. Moulijn, Direct Epoxidation of Propene Using Gold Dispersed on TS-1 and Other Titanium-Containing Supports, Industrial & Engineering Chemistry Research, 38 (1999) 884-891.
[98] B. Taylor, J. Lauterbach, G.E. Blau, W.N. Delgass, Reaction Kinetic Analysis of the Gas-Phase Epoxidation of Propylene over Au/TS-1, Journal of Catalysis, 242 (2006) 142-152.
[99] E.E. Stangland, B. Taylor, R.P. Andres, W.N. Delgass, Direct Vapor Phase Propylene Epoxidation over Deposition-Precipitation Gold-Titania Catalysts in the Presence of H2/O2: Effects of Support, Neutralizing Agent, and Pretreatment, Journal of Physical Chemistry B, 109 (2005) 2321-2330.
[100] D.T. Bregante, N.E. Thornburg, J.M. Notestein, D.W. Flaherty, Consequences of Confinement for Alkene Epoxidation with Hydrogen Peroxide on Highly Dispersed Group 4 and 5 Metal Oxide Catalysts, ACS Catalysis, 8 (2018) 2995-3010.
[101] D.S. Potts, C. Torres, O. Kwon, D.W. Flaherty, Engineering intraporous solvent environments: effects of aqueous-organic solvent mixtures on competition between zeolite-catalyzed epoxidation and H_2O_2 decomposition pathways, Chemical Science, 14 (2023) 3160-3181.
[102] C. Torres, D.S. Potts, D.W. Flaherty, Solvent Mediated Interactions on Alkene Epoxidations in Ti-MFI: Effects of Solvent Identity and Silanol Density, ACS Catalysis, 13 (2023) 8925-8942.
[103] J. Goetze, I. Yarulina, J. Gascon, F. Kapteijn, B.M. Weckhuysen, Revealing Lattice Expansion of Small-Pore Zeolite Catalysts during the Methanol-to-Olefins Process Using Combined Operando X-ray Diffraction and UV–vis Spectroscopy, ACS Catalysis, 8 (2018) 2060-2070.
[104] W. He, D.S. Potts, Z. Zhang, B. Liu, R.L. Schuarca, S.-J. Hwang, J.Q. Bond, D.W. Flaherty, V.J. Cybulskis, Lewis acidity and substituent effects influence aldehyde enolization and C–C coupling in beta zeolites, Journal of Catalysis, 427 (2023) 115105.
[105] G. Valerio, J. Plévert, A. Goursot, F.d. Renzo, Modeling of boron substitution in zeolites and implications on lattice parameters, Physical Chemistry Chemical Physics, 2 (2000) 1091-1094.

[106] A.R. Maag, G.A. Tompsett, J. Tam, C.A. Ang, G. Azimi, A.D. Carl, X. Huang, L.J. Smith, R.L. Grimm, J.Q. Bond, M.T. Timko, ZSM-5 decrystallization and dealumination in hot liquid water, Physical Chemistry Chemical Physics, 21 (2019) 17880-17892.
[107] P.A. Zapata, Y. Huang, M.A. Gonzalez-Borja, D.E. Resasco, Silylated hydrophobic zeolites with enhanced tolerance to hot liquid water, Journal of Catalysis, 308 (2013) 82-97.
[108] A.L. Patterson, The Scherrer Formula for X-Ray Particle Size Determination, Physical Review, 56 (1939) 978-982.
[109] L.G. Parratt, Surface Studies of Solids by Total Reflection of X-Rays, Physical Review, 95 (1954) 359-369.
[110] J. Liu, R.E. Saw, Y.H. Kiang, Calculation of Effective Penetration Depth in X-Ray Diffraction for Pharmaceutical Solids, J. Pharm. Sci., 99 (2010) 3807-3814.
[111] FIZ-Karlsruhe, (2023). Inorganic Crystal Structure Database, https://icsd.products.fiz-karlsruhe.de. Accessed: November 22, 2023.
[112] K. Momma, F. Izumi, VESTA 3 for three-dimensional visualization of crystal, volumetric and morphology data, Journal of Applied Crystallography, 44 (2011) 1272-1276.
[113] J. Lipp, R. Banerjee, M.F. Patwary, N. Patra, A. Dong, F. Girgsdies, S.R. Bare, J.R. Regalbuto, Extension of Rietveld Refinement for Benchtop Powder XRD Analysis of Ultrasmall Supported Nanoparticles, Chemistry of Materials, 34 (2022) 8091-8111.
[114] K. O'Connell, J.R. Regalbuto, High Sensitivity Silicon Slit Detectors for 1 nm Powder XRD Size Detection Limit, Catalysis Letters, 145 (2015) 777-783.
[115] F. Bertolotti, D. Moscheni, A. Guagliardi, N. Masciocchi, When Crystals Go Nano – The Role of Advanced X-ray Total Scattering Methods in Nanotechnology, European Journal of Inorganic Chemistry, 2018 (2018) 3789-3803.
[116] B.E. Spiewak, B.E. Handy, S.B. Sharma, J.A. Dumesic, Microcalorimetric studies of ammonia adsorption on γ-Al_2O_3, HNa-Y zeolite, and H-mordenite, Catalysis Letters, 23 (1994) 207-213.
[117] G. Cucinieri Colorio, A. Auroux, B. Bonnetot, Acidity and surface behaviour of alumina-boria catalysts studied by adsorption microcalorimetry of probe molecules, Journal of Thermal Analysis, 40 (1993) 1267-1276.
[118] D.R. Aireddy, K. Ding, Heterolytic Dissociation of H_2 in Heterogeneous Catalysis, ACS Catalysis, 12 (2022) 4707-4723.
[119] A.B. Kellicutt, R. Salary, O.A. Abdelrahman, J.Q. Bond, An examination of the intrinsic activity and stability of various solid acids during the catalytic decarboxylation of γ-valerolactone, Catalysis Science & Technology, 4 (2014) 2267-2279.
[120] J.G. Tittensor, R.J. Gorte, D.M. Chapman, Isopropylamine adsorption for the characterization of acid sites in silica-alumina catalysts, Journal of Catalysis, 138 (1992) 714-720.
[121] S.G. Wettstein, J.Q. Bond, D.M. Alonso, H.N. Pham, A.K. Datye, J.A. Dumesic, RuSn bimetallic catalysts for selective hydrogenation of levulinic acid to γ-valerolactone, Applied Catalysis B: Environmental, 117-118 (2012) 321-329.
[122] R. Haul, G. Neubauer, Kinetic studies on the mechanism of the catalytic ethene oxidation, Journal of Catalysis, 105 (1987) 39-54.
[123] J.A. Mahoney, The use of a gradientless reactor in petroleum reaction engineering studies, Journal of Catalysis, 32 (1974) 247-253.

[124] V.J. Cybulskis, A.D. Smeltz, Y. Zvinevich, R. Gounder, W.N. Delgass, F.H. Ribeiro, Learning the Fundamentals of Kinetics and Reaction Engineering with the Catalytic Oxidation of Methane, Chemical Engineering Education, 50 (2016) 202-210.
[125] S.C. Paspek, A. Varma, J.J. Carberry, Utilization of the Recycle Reactor in Determining Kinetics of Gas-Solid Catalytic Reactions, Chemical Engineering Education, 14 (1980) 78-82.
[126] R.A. Demmin, R.J. Gorte, Design parameters for temperature-programmed desorption from a packed bed, Journal of Catalysis, 90 (1984) 32-39.
[127] I.E. Wachs, B.M. Weckhuysen, Structure and reactivity of surface vanadium oxide species on oxide supports, Applied Catalysis A: General, 157 (1997) 67-90.
[128] P. Hollins, The influence of surface defects on the infrared spectra of adsorbed species, Surface Science Reports, 16 (1992) 51-94.
[129] E. Bus, J.T. Miller, A.J. Kropf, R. Prins, J.A. van Bokhoven, Analysis of in situ EXAFS data of supported metal catalysts using the third and fourth cumulant, Physical Chemistry Chemical Physics, 8 (2006) 3248-3258.
[130] M. Newville, Fundamentals of XAFS, Reviews in Mineralogy and Geochemistry, 78 (2014) 33-74.
[131] J.D. Lewis, M. Ha, H. Luo, A. Faucher, V.K. Michaelis, Y. Román-Leshkov, Distinguishing Active Site Identity in Sn-Beta Zeolites Using 31P MAS NMR of Adsorbed Trimethylphosphine Oxide, ACS Catalysis, 8 (2018) 3076-3086.
[132] W.R. Gunther, V.K. Michaelis, R.G. Griffin, Y. Román-Leshkov, Interrogating the Lewis Acidity of Metal Sites in Beta Zeolites with ^{15}N Pyridine Adsorption Coupled with MAS NMR Spectroscopy, Journal of Physical Chemistry C, 120 (2016) 28533-28544.
[133] I.E. Wachs, C.A. Roberts, Monitoring surface metal oxide catalytic active sites with Raman spectroscopy, Chemical Society Reviews, 39 (2010) 5002-5017.
[134] V.J. Cybulskis, J. Wang, J.H. Pazmiño, F.H. Ribeiro, W.N. Delgass, Isotopic Transient Studies of Sodium Promotion of Pt/Al_2O_3 for the Water–Gas Shift Reaction, Journal of Catalysis, 339 (2016) 163-172.
[135] J. Wang, V.F. Kispersky, W. Nicholas Delgass, F.H. Ribeiro, Determination of the Au Active Site and Surface Active Species via Operando Transmission FTIR and Isotopic Transient Experiments on 2.3wt.% Au/TiO_2 for the WGS Reaction, Journal of Catalysis, 289 (2012) 171-178.
[136] X. Gao, I.E. Wachs, Investigation of Surface Structures of Supported Vanadium Oxide Catalysts by UV−vis−NIR Diffuse Reflectance Spectroscopy, Journal of Physical Chemistry B, 104 (2000) 1261-1268.
[137] E.I. Ross-Medgaarden, I.E. Wachs, Structural Determination of Bulk and Surface Tungsten Oxides with UV−vis Diffuse Reflectance Spectroscopy and Raman Spectroscopy, Journal of Physical Chemistry C, 111 (2007) 15089-15099.
[138] P. Makuła, M. Pacia, W. Macyk, How To Correctly Determine the Band Gap Energy of Modified Semiconductor Photocatalysts Based on UV–Vis Spectra, Journal of Physical Chemistry Letters, 9 (2018) 6814-6817.
[139] J. Manikantan, H.B. Ramalingam, B.C. Shekar, B. Murugan, R.R. Kumar, J.S. Santhoshi, Physical and optical properties of HfO_2 NPs – Synthesis and characterization in finding its feasibility in opto-electronic devices, Advanced Powder Technology, 28 (2017) 1636-1646.

[140] A. Ramadoss, K. Krishnamoorthy, S.J. Kim, Novel synthesis of hafnium oxide nanoparticles by precipitation method and its characterization, Materials Research Bulletin, 47 (2012) 2680-2684.
[141] D.T. Bregante, D.S. Potts, O. Kwon, E.Z. Ayla, J.Z. Tan, D.W. Flaherty, Effects of Hydrofluoric Acid Concentration on the Density of Silanol Groups and Water Adsorption in Hydrothermally Synthesized Transition-Metal-Substituted Silicalite‐1, Chemistry of Materials, (2020) 1 - 13.
[142] T. Blasco, A. Corma, M.T. Navarro, J.P. Pariente, Synthesis, Characterization, and Catalytic Activity of Ti-MCM-41 Structures, Journal of Catalysis, 156 (1995) 65-74.
[143] D.A. Hickman, J.C. Degenstein, F.H. Ribeiro, Fundamental principles of laboratory fixed bed reactor design, Current Opinion in Chemical Engineering, 13 (2016) 1-9.
[144] P.B. Weisz, C.D. Prater, Interpretation of Measurements in Experimental Catalysis, in: W.G. Frankenburg, V.I. Komarewsky, E.K. Rideal (Eds.) Advances in Catalysis, Academic Press, 1954, pp. 143-196.
[145] D.E. Mears, On Criteria for Axial Dispersion in Nonisothermal Packed-Bed Catalytic Reactors, Industrial & Engineering Chemistry Fundamentals, 15 (1976) 20-23.
[146] K.S.W. Sing, Reporting physisorption data for gas/solid systems with special reference to the determination of surface area and porosity (Recommendations 1984), Pure and Applied Chemistry, 57 (1985) 603-619.
[147] J.R. Anderson, Structure of Metallic Catalysts, 1st ed., Academic Press, 1975.
[148] T. Islamoglu, K.B. Idrees, F.A. Son, Z. Chen, S.-J. Lee, P. Li, O.K. Farha, Are you using the right probe molecules for assessing the textural properties of metal–organic frameworks?, Journal of Materials Chemistry A, 10 (2022) 157-173.
[149] G.U. Rakhmatkariev, A.J. Palace Carvalho, J.P. Prates Ramalho, Adsorption of Normal Pentane on the Surface of Rutile. Experimental Results and Simulations, Langmuir, 23 (2007) 7555-7561.
[150] L. Liu, S. Tan, T. Horikawa, D.D. Do, D. Nicholson, J. Liu, Water adsorption on carbon - A review, Advances in Colloid and Interface Science, 250 (2017) 64-78.
[151] F. Rouquerol, J. Rouquerol, K. Sing, Adsorption by Powders and Porous Solids: Principles, Methodology and Applications 1st ed., Academic Press, San Diego, CA, London, 1999.
[152] J.E.S. S. Lowell, Martin A. Thomas, Matthias Thommes, Characterization of Porous Solids and Powders: Surface Area, Pore Size and Density, 1st ed., Kluwer Academic Publishers, Dordrecht, The Netherlands, 2004.
[153] K. Nakai, J. Sonoda, M. Yoshida, M. Hakuman, H. Naono, High resolution adsorption isotherms of N2 and Ar for nonporous silicas and MFI zeolites, Adsorption, 13 (2007) 351-356.
[154] J. Jagiello, J. Kenvin, NLDFT adsorption models for zeolite porosity analysis with particular focus on ultra-microporous zeolites using O_2 and H_2, Journal of Colloid and Interface Science, 625 (2022) 178-186.
[155] Micromeritics, (2023). Tech Tip 14: Minimum Surface Area Measurements with Micromeritics Physisorption Analyzers, https://www.micromeritics.com/Repository/Files/micro_tech_tip_14-surface-area-analyses.pdf. Accessed: November 27, 2023.
[156] J. Medema, J.P.W. Houtman, Brunauer-Emmett-Teller specific measurement of solids using krypton, Analytical Chemistry, 41 (1969) 209-211.

[157] M. Thommes, K.A. Cychosz, A.V. Neimark, Chapter 4 - Advanced Physical Adsorption Characterization of Nanoporous Carbons, in: J.M.D. Tascón (Ed.) Novel Carbon Adsorbents, Elsevier, Oxford, 2012, pp. 107-145.
[158] P.I. Ravikovitch, A. Vishnyakov, R. Russo, A.V. Neimark, Unified Approach to Pore Size Characterization of Microporous Carbonaceous Materials from N_2, Ar, and CO_2 Adsorption Isotherms, Langmuir, 16 (2000) 2311-2320.
[159] A.J. Howarth, A.W. Peters, N.A. Vermeulen, T.C. Wang, J.T. Hupp, O.K. Farha, Best Practices for the Synthesis, Activation, and Characterization of Metal–Organic Frameworks, Chemistry of Materials, 29 (2017) 26-39.
[160] M. Thommes, K. Kaneko, A.V. Neimark, J.P. Olivier, F. Rodriguez-Reinoso, J. Rouquerol, K.S.W. Sing, Physisorption of gases, with special reference to the evaluation of surface area and pore size distribution (IUPAC Technical Report), Pure and Applied Chemistry, 87 (2015) 1051-1069.
[161] S. Brunauer, P.H. Emmett, E. Teller, Adsorption of Gases in Multimolecular Layers, Journal of the American Chemical Society, 60 (1938) 309-319.
[162] W.G. McMillan, E. Teller, The Assumptions of the B.E.T. Theory, Journal of Physical Chemistry, 55 (1951) 17-20.
[163] K.D. Hammond, W.C. Conner, Chapter One - Analysis of Catalyst Surface Structure by Physical Sorption, in: B.C. Gates, F.C. Jentoft (Eds.) Advances in Catalysis, Academic Press, 2013, pp. 1-101.
[164] Y.-S. Bae, A.Ö. Yazaydın, R.Q. Snurr, Evaluation of the BET Method for Determining Surface Areas of MOFs and Zeolites that Contain Ultra-Micropores, Langmuir, 26 (2010) 5475-5483.
[165] S. Storck, H. Bretinger, W.F. Maier, Characterization of micro- and mesoporous solids by physisorption methods and pore-size analysis, Applied Catalysis A: General, 174 (1998) 137-146.
[166] J. Jagiello, W. Betz, Characterization of pore structure of carbon molecular sieves using DFT analysis of Ar and H_2 adsorption data, Microporous and Mesoporous Materials, 108 (2008) 117-122.
[167] Micromeritics, (2023). DFT / NLDFT Density Functional Theory, https://www.micromeritics.com/resources/dft-nldft-density-functional-theory/. Accessed: November 27, 2023.
[168] H. Giesche, Mercury Porosimetry: A General (Practical) Overview, Particle & Particle Systems Characterization, 23 (2006) 9-19.
[169] ASTM, (2017). D4284-12(2017)e1 Standard Test Method for Determining Pore Volume Distribution of Catalysts and Catalyst Carriers by Mercury Intrusion Porosimetry, West Conshohocken, PA, pp. 1-7.
[170] J. Rouquerol, G. Baron, R. Denoyel, H. Giesche, J. Groen, P. Klobes, P. Levitz, A.V. Neimark, S. Rigby, R. Skudas, K. Sing, M. Thommes, K. Unger, Liquid intrusion and alternative methods for the characterization of macroporous materials (IUPAC Technical Report), Pure and Applied Chemistry, 84 (2011) 107-136.
[171] ASTM, (2021). D8393-21 Standard Guide for Determination of Pore Volume of Powdered Catalysts and Catalyst Carriers by Water Adsorption, West Conshohocken, PA, pp. 1-4.

[172] H.G.T. Nguyen, J.C. Horn, M. Bleakney, D.W. Siderius, L. Espinal, Understanding Material Characteristics through Signature Traits from Helium Pycnometry, Langmuir, 35 (2019) 2115-2122.
[173] J.B. Wade, G.P. Martin, D.F. Long, An assessment of powder pycnometry as a means of determining granule porosity, Pharmaceutical Development and Technology, 20 (2015) 257-265.
[174] M. Shekhar, J. Wang, W.-S. Lee, W.D. Williams, S.M. Kim, E.A. Stach, J.T. Miller, W.N. Delgass, F.H. Ribeiro, Size and Support Effects for the Water–Gas Shift Catalysis over Gold Nanoparticles Supported on Model Al_2O_3 and TiO_2, Journal of the American Chemical Society, 134 (2012) 4700-4708.
[175] R.J. Matyi, L.H. Schwartz, J.B. Butt, Particle Size, Particle Size Distribution, and Related Measurements of Supported Metal Catalysts, Catalysis Reviews, 29 (1987) 41-99.
[176] P.L. Gai, E.D. Boyes, Electron Microscopy in Heterogeneous Catalysis, 1st ed., CRC Press, Boca Raton, 2003.
[177] S.J. Pennycook, P.D. Nellist, Scanning Transmission Electron Microscopy: Imaging and Analysis, 1st ed., Springer, New York Dordrecht Heidelberg London, 2011.
[178] I. Alxneit, Particle Size Distributions from Electron Microscopy Images: Avoiding Pitfalls, The Journal of Physical Chemistry A, 124 (2020) 10075-10081.
[179] A.K. Datye, Q. Xu, K.C. Kharas, J.M. McCarty, Particle size distributions in heterogeneous catalysts: What do they tell us about the sintering mechanism?, Catalysis Today, 111 (2006) 59-67.
[180] ASTM, (2022). D4513-22 Standard Test Method for Particle Size Distribution of Catalytic Materials by Sieving, West Conshohocken, PA, pp. 1-3.
[181] R. Xu, Particle Characterization: Light Scattering Methods, 1st ed., Kluwer Academic Publishers, New York, Boston, Dordrecht, London, Moscow, 2002.
[182] ASTM, (2020). D4464-15(2020) Standard Test Method for Particle Size Distribution of Catalytic Materials by Laser Light Scattering, West Conshohocken, PA, pp. 1-5.
[183] Calgonate, (2023). HF Safety Information, https://www.calgonate.com/safety_info.php. Accessed: November 28, 2023.
[184] H. Robson, Chapter 8 - Safety considerations for zeolite synthesis, in: H. Robson, K.P. Lillerud (Eds.) Verified Syntheses of Zeolitic Materials, Elsevier Science, Amsterdam, 2001, pp. 45-46.
[185] N.N. Greenwood, A. Earnshaw, Chemistry of the Elements, 2nd ed., Elsevier; Butterworth-Heinemann, Oxford, 1997.
[186] InorganicVentures, (2023). Sample Preparation Guide, https://www.inorganicventures.com/sample-preparation-guide. Accessed: November 28, 2023.
[187] ASTM, (2012). UOP961-12 Elemental Composition of Zeolites by ICP-OES, West Conshohocken, PA, pp. 1-12.
[188] M. Fadoni, L. Lucarelli, Temperature programmed desorption, reduction, oxidation and flow chemisorption for the characterisation of heterogeneous catalysts. Theoretical aspects, instrumentation and applications, Stud Surf Sci Catal, 120 (1999) 177-225.
[189] J. Wang, B. McEnaney, Quantitative calibration of a TPD-MS system for CO and CO_2 using calcium carbonate and calcium oxalate, Thermochimica Acta, 190 (1991) 143-153.

[190] F.C. Jentoft, Chapter 3 Ultraviolet–Visible–Near Infrared Spectroscopy in Catalysis: Theory, Experiment, Analysis, and Application Under Reaction Conditions, in: Advances in Catalysis, Academic Press, 2009, pp. 129-211.
[191] A.T. Bell, NMR Techniques in Catalysis, 1st ed., CRC Press, Boca Raton, 1994.
[192] ASTM, (2020). D4222-20 Standard Test Method for Determination of Nitrogen Adsorption and Desorption Isotherms of Catalysts and Catalyst Carriers by Static Volumetric Measurements, West Conshohocken, PA, pp. 1-6.

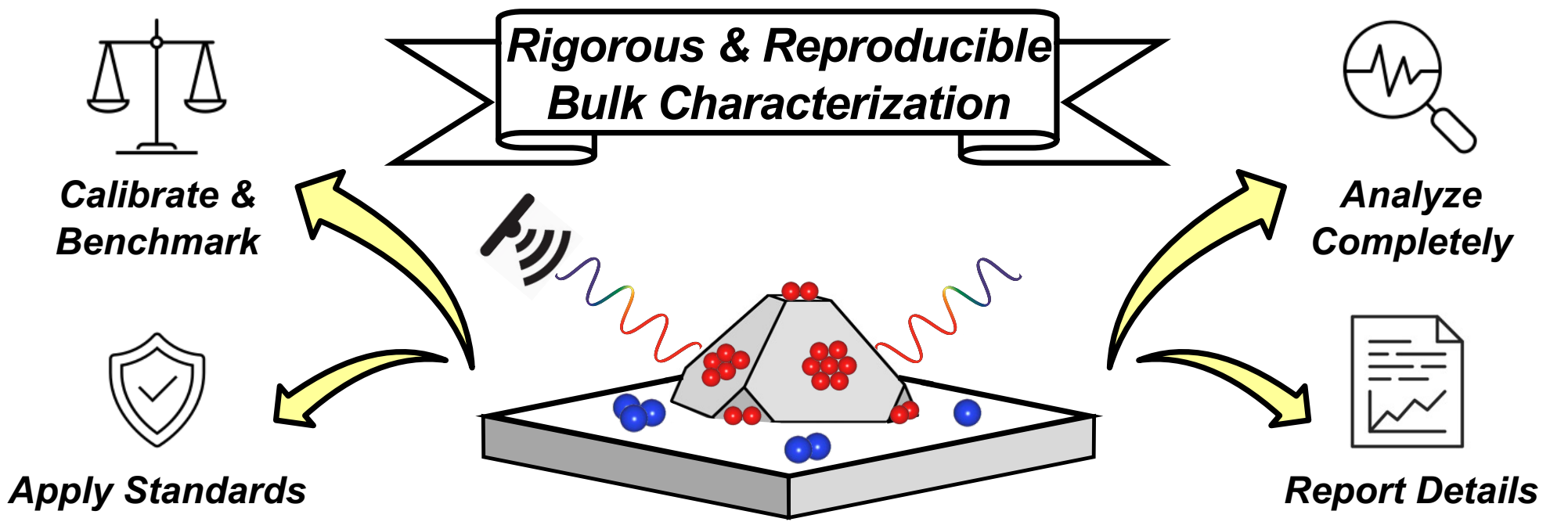
Rigorous & Reproducible
Bulk Characterization
Calibrate &
Benchmark
Analyze
Completely
Apply Standards
Report Details